

# Single-Molecule Fluorescence Resonance Energy Transfer Investigations of Ribosome-Catalyzed Protein Synthesis

Daniel D. MacDougall

Jingyi Fei

Ruben L. Gonzalez, Jr.

## I. INTRODUCTION

Protein synthesis, or translation, is an inherently dynamic process in which the ribosome traverses the open reading frame of a messenger RNA (mRNA) template in steps of precisely one triplet-nucleotide codon, catalyzing the selection of aminoacyl-transfer RNA (aa-tRNA) substrates and polymerization of the nascent polypeptide chain, while simultaneously coordinating the sequential binding of exogenous translation factors. The complexity of this process is mirrored by the intricate molecular architecture of the ribosome itself, highlighted in atomic detail by recent X-ray crystallographic structures that reveal an elaborate network of RNA-RNA, RNA-protein, and protein-protein interactions (Korostelev and Noller, 2007; Steitz, 2008). This high degree of intra- and inter-molecular connectivity suggests that allosteric mechanisms may regulate the activity and coordinate the timing of biochemical events catalyzed by spatially distal ribosomal functional centers. Large-scale conformational dynamics of the ribosome have similarly been implicated as a means by which to regulate the biochemical steps of protein synthesis and to power forward progression through the kinetic steps of the translation process.

Comparison of X-ray crystallographic structures of ribosomal subunits as well as the intact ribosome in the absence and presence of translation factors (reviewed in Schmeing and Ramakrishnan [2009]), together with the analysis of cryogenic electron microscopy (cryo-EM) reconstructions of the ribosome trapped at various functional states during protein synthesis (see Chapter 7), has allowed visualization of large-scale conformational rearrangements of the translational machinery. Through such comparative structural analysis, mobile ribosomal domains have been identified and specific conformational changes have been inferred. However, these static structural images lack information regarding the timescales of the inferred

conformational changes, and the kinetic and thermodynamic parameters underlying the corresponding ribosomal motions. Such dynamic information has recently been uncovered through the application of single-molecule fluorescence resonance energy transfer (smFRET) to studies of protein synthesis. This technique has proven to be particularly well-suited for monitoring and characterizing large-scale conformational dynamics of the ribosome and its tRNA and translation factor ligands, which often occur on length scales ( $\sim$ tens of Å) and time scales ( $\sim$ ms to s) that are well matched with the spatio-temporal resolution of current smFRET methodologies (see Chapter 1). Guided by the structural data, numerous donor-acceptor fluorophore labeling schemes have already been developed, each capable of monitoring specific conformational changes of the translational machinery in real time.

In this chapter, we will first briefly discuss experimental considerations pertaining to the design and implementation of smFRET investigations of highly purified *in vitro* translation systems (Section II). We then describe some of the major findings from smFRET studies of Bacterial protein synthesis, highlighting emergent themes and single-molecule-specific insights that have been gleaned (Sections III–V). A majority of the literature to date has focused on events occurring during the elongation phase of translation, and primarily during the aa-tRNA selection and translocation steps of the translation elongation cycle; accordingly, we confine the bulk of our discussion to the conformational dynamics of the translational machinery that are pertinent to aa-tRNA selection and translocation. Specifically, in Section III, we discuss pre-steady state and steady-state smFRET measurements of aa-tRNA selection, which have allowed observation and characterization of the conformational trajectory of aa-tRNA as it is selected and accommodated into the ribosomal A site, revealing a crucial intermediate that had previously evaded biochemical

detection and has thus far eluded structural characterization due to its transient nature. Section IV focuses on steady-state investigations of translocation-relevant conformational equilibria, which have led to the discovery that many of the conformational rearrangements associated with translocation occur spontaneously and reversibly upon peptide bond formation, with the ribosome possessing the intrinsic capability of accessing functionally relevant conformational states through thermal fluctuations alone. The ability of translation factors and antibiotics to modulate these equilibria – through the manipulation of transition rates and stabilization/destabilization of particular conformational states – can be directly observed and correlated with their ability to promote or inhibit translocation, respectively. Finally, in Section V, we discuss recent smFRET investigations that have extended these ideas to the initiation, termination, and ribosome recycling stages of protein synthesis, providing evidence that modulation of intrinsic ribosomal dynamics and conformational equilibria represents a common regulatory mechanism used by translation factors during all stages of protein synthesis. A dynamic picture of the translating ribosome emerges in which thermal fluctuations drive spontaneous ribosome and tRNA motions that form the basis for ribosome function. Addition of translation factors to this mechanistic foundation provides a means by which to modulate, accelerate, guide the directionality, and increase the efficiency of these intrinsic processes, thereby accomplishing highly regulated and tightly controlled protein synthesis.

## II. DESIGN OF smFRET EXPERIMENTS

### II.1 Site-Specific Fluorescent Labeling of Translation Components

Preparation of fluorescently labeled translation components is the starting point for any smFRET investigation of ribosome conformational dynamics (Fei et al., 2010). Donor and acceptor fluorophore pairs can be conjugated to tRNAs, translation factors, the ribosome, or any combination thereof, with the choice of labeled components depending on the particular molecular interaction(s) or conformational rearrangement(s) to be monitored. The design of a mechanistically informative labeling scheme relies heavily on X-ray crystallographic and cryo-EM structural models, which are used to choose labeling positions that will allow sensitive detection of the conformational change of interest without perturbing biochemical activity. Site-specific labeling of translation components is critical for being able to interpret changes in FRET efficiency in molecular detail as corresponding to movement of a particular ribosomal domain or the formation of a particular inter-molecular interaction. Consequently, numerous labeling strategies have been developed, which have helped to increase the scope of smFRET studies of ribosome

conformational dynamics, allowing researchers to probe various structural transitions.

Donor and acceptor fluorophores have been covalently attached to tRNA species at naturally occurring, post-transcriptionally modified nucleotides within the molecule's central elbow region, or to the amino acid linked to the 3'-terminal aminoacyl acceptor stem of the tRNA (Sytnik et al., 1999; Blanchard et al., 2004b). Translation factors can be fluorescently labeled at unique cysteine residues or unnatural amino acids that have been incorporated at appropriate positions on the molecule's surface (Wang et al., 2007; Munro et al., 2009b; Sternberg et al., 2009). Fluorescent labeling of the ribosome itself has been achieved by two major approaches. In the first, purified ribosomal proteins (r-proteins) are fluorescently labeled and subsequently reconstituted *in vitro* with ribosomal subunits (Hickerson et al., 2005; Fei et al., 2009). In the second approach, helical extensions engineered into ribosomal RNA (rRNA) stem-loops are hybridized to a complementary fluorescently labeled oligonucleotide (Dorywalska et al., 2005).

### II.2 Surface Immobilization of Ribosomal Complexes and smFRET Imaging

Once fluorescently labeled translation components have been prepared and their biochemical activities have been confirmed to be unimpaired by labeling, smFRET imaging typically requires immobilization of ribosomal complexes on the surface of a polymer-passivated microscope slide. Quartz microscope slides can be passivated with a mixture of polyethylene glycol (PEG) and biotin-PEG (Ha et al., 2002), thereby allowing specific attachment of biotinylated ribosomal complexes through a biotin-streptavidin-biotin linkage (Blanchard et al., 2004b). Most frequently, ribosomal complexes are assembled on a 5'-biotinylated mRNA molecule (or a 3'-biotinylated oligonucleotide hybridized to the mRNA 5' end), which serves as the attachment point between ribosome and surface (Figure 6.1). An alternative approach has been reported whereby the 3' end of the large 50S subunit 23S rRNA can be oxidized, biotinylated, and used as the anchor point (Stapulionis et al., 2008).

Stable attachment of fluorescently labeled ribosomal complexes to the slide surface permits acquisition of smFRET versus time trajectories from single ribosomes, with an observation time (seconds to minutes) that is often limited by photobleaching of the organic fluorophores. Total internal reflection (TIR) illumination is generally used for excitation of donor fluorophores within single ribosomal complexes; when combined with wide-field imaging, this approach allows acquisition of smFRET versus time data from hundreds of ribosomal complexes simultaneously (see Chapter 1). Importantly, the biochemical activities of ribosomes immobilized using the methods described

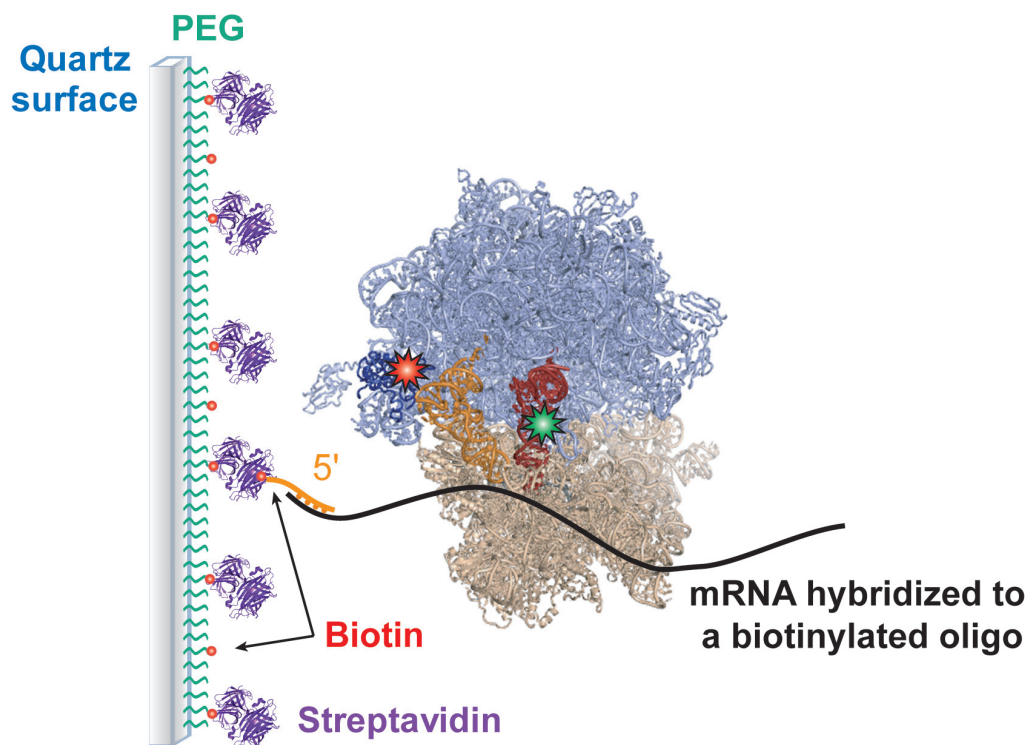


**FIGURE 6.1: Surface immobilization strategy.** Quartz flow cells are first passivated with a mixture of PEG and biotin-PEG. This passivated flow cell is incubated with streptavidin prior to use. Fluorescently labeled ribosomal complexes are immobilized on the surface via a biotin-streptavidin-biotin interaction.

in the previous paragraph remain intact; surface-tethered ribosomes have been demonstrated to be active in the individual steps of translation initiation (Marshall et al., 2008; Marshall et al., 2009), elongation (Blanchard et al., 2004b; Stapulionis et al., 2008), termination, and ribosome recycling (Sternberg et al., 2009).

### III. AMINOACYL-tRNA SELECTION

#### III.1 Selection of aa-tRNA by the Ribosome

During each elongation cycle in protein synthesis, an aa-tRNA is delivered to the ribosome in a “ternary complex” with elongation factor Tu (EF-Tu) and GTP. Based on biochemical experiments, a kinetic model has been formulated that details the stepwise progression of aa-tRNA into the ribosomal A site during aa-tRNA selection, culminating in accommodation of aa-tRNA into the peptidyl transferase center and peptide bond formation (reviewed in Rodnina et al. [2005]). One of the first applications of smFRET to the study of protein synthesis allowed direct visualization of aa-tRNA selection by the ribosome, using fluorophore-labeled tRNAs as FRET probes to follow the conformational trajectory of the incoming aa-tRNA in real time (Blanchard et al., 2004a). This study added important mechanistic details to our understanding of how the ribosome rapidly and efficiently selects the correct

aa-tRNA, thereby ensuring faithful incorporation of the mRNA-encoded amino acid into the growing polypeptide chain, and highlighted the role of aa-tRNA dynamics in the selection process.

Selection of the cognate (correct) aa-tRNA from a pool of competitor near-cognate (one mismatch at a non-wobble position) and non-cognate (at least two mismatches) aa-tRNAs is performed rapidly and efficiently by the ribosome, with an error rate of approximately 1 out of every 1,000 to 10,000 amino acids incorporated into the polypeptide (Parker, 1989). Such a high level of discrimination between correct and incorrect aa-tRNAs, which can differ by as little as a single Watson-Crick base pair within the codon-anticodon duplex, cannot be explained based solely on differences in the free energy of codon-anticodon formation (Grosjean et al., 1978). Biochemical experiments have shed light on the mechanisms through which the ribosome can achieve such a high degree of selectivity. A kinetic proofreading strategy is exploited whereby the ribosome discriminates in favor of cognate aa-tRNAs at two independent selection steps termed “initial selection” and “proofreading,” which are separated by the chemical step of GTP hydrolysis (Hopfield, 1974; Thompson and Stone, 1977). Furthermore, during both initial selection and proofreading, induced-fit mechanisms act to preferentially select for the cognate aa-tRNA (reviewed in Daviter et al. [2006]). Correct base pairing of the codon-anticodon duplex within

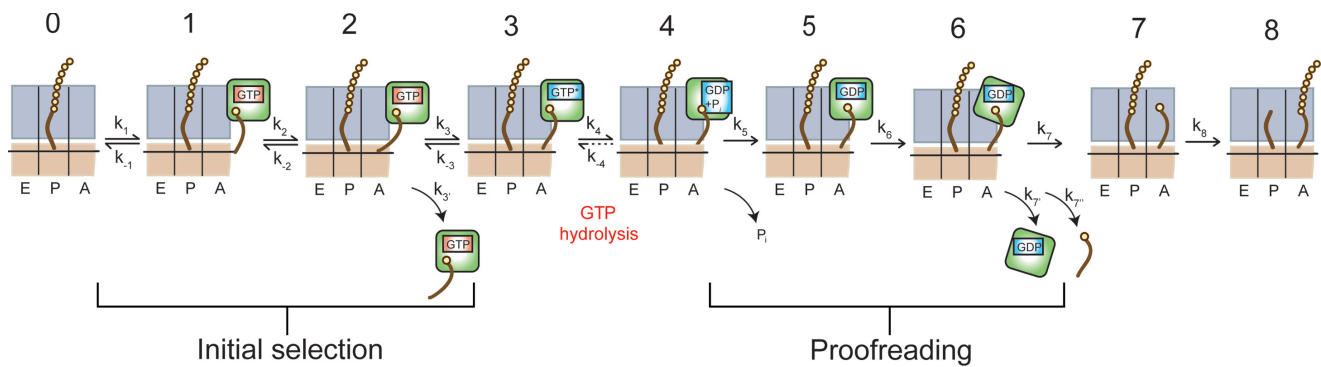


**FIGURE 6.2: Kinetic model for aa-tRNA selection.** Step 0→1: Initial binding of the EF-Tu(GTP)aa-tRNA ternary complex to the ribosome via interactions between EF-Tu and the L7/L12 stalk. Step 1→2: Formation of codon-anticodon interaction at the decoding center on the 30S subunit. Step 2→3: GTPase activation. At this stage, the ternary complex can either dock into the GTPase center on the 50S subunit ( $k_3$ ) or be rejected from the ribosome ( $k_3'$ ). Step 3→4: GTP hydrolysis by EF-Tu. Step 4→5: Release of  $P_i$  from EF-Tu. Step 5→6: EF-Tu conformational change from its GTP-bound form to its GDP-bound form. Step 6→7: aa-tRNA is released from EF-Tu, which dissociates from the ribosome ( $k_7$ ). aa-tRNA can either accommodate into the peptidyl transferase center ( $k_7$ ) or be rejected and dissociate from the ribosome ( $k_7''$ ). Step 7→8: Peptidyl transfer between P- and A-site tRNAs ( $k_8$ ). Figure adapted from Frank and Gonzalez (2010), copyright © 2010 Annual Reviews.

the small 30S ribosomal subunit's decoding center induces specific conformational rearrangements of the tRNA and ribosome that accelerate its forward progression through the reaction pathway compared to non- or near-cognate aa-tRNAs.

The detailed kinetic model for aa-tRNA selection by the ribosome is depicted schematically in Figure 6.2 (for a review, see Rodnina and Wintermeyer [2001]). The ternary complex initially binds to the ribosome through protein-protein interactions between EF-Tu and the ribosomal L7/L12 stalk ( $k_1/k_{-1}$ ), followed by formation of the codon-anticodon interaction within the 30S ribosomal subunit's decoding center ( $k_2/k_{-2}$ ). Subsequent GTPase activation of EF-Tu ( $k_3$ ), which is rate-limiting for GTP hydrolysis ( $k_4$ ), is selectively accelerated in response to recognition of a cognate codon-anticodon interaction through an induced-fit mechanism. Non- and near-cognate aa-tRNAs, in contrast, have a lower probability of advancing past this initial selection step as a result of a lower rate of GTPase activation (slower  $k_3$ ) as well as an increased rate of ternary complex dissociation (faster  $k_3'$ ), owing to weaker interactions with the ribosome. These effects lead to near-complete discrimination against non-cognate aa-tRNAs during initial selection. Following GTPase activation and GTP hydrolysis by EF-Tu, inorganic phosphate ( $P_i$ ) is released ( $k_5$ ), EF-Tu undergoes a conformational change to its GDP-bound form ( $k_6$ ), and ultimately dissociates from the ribosome ( $k_7$ ). The GDP-bound form of EF-Tu has a low affinity for aa-tRNA; consequently, the 3'-terminus of the aa-tRNA is released, and the aa-tRNA may either be accommodated into the peptidyl-transferase center of the 50S ribosomal subunit ( $k_7$ ) to form a peptide bond ( $k_8$ ) or be rejected from the ribosome ( $k_7''$ ). An induced-fit mechanism operates during this proofreading step of aa-tRNA selection by accelerating the rate of accommodation in response to a

cognate, but not a near-cognate, codon-anticodon interaction. In addition, the rate of dissociation ( $k_7''$ ) is faster for more weakly bound near-cognate aa-tRNAs, further decreasing the probability that they will be accommodated into the peptidyl transferase center and allowed to participate in peptide bond formation.

### III.2 Real-Time smFRET Observation of aa-tRNA Selection

smFRET studies of aa-tRNA selection were designed and interpreted within the biochemical framework described in the previous section. The selection and incorporation of aa-tRNA into single ribosomes was followed by monitoring the time evolution of smFRET upon delivery of acceptor-labeled EF-Tu(GTP)Phe-tRNA<sup>Phe</sup> ternary complex (labeled with a Cy5 acceptor fluorophore at the acp<sup>3</sup>U47 residue within tRNA<sup>Phe</sup>) to surface-immobilized ribosomal initiation complexes bearing donor-labeled fMet-tRNA<sup>fMet</sup> (labeled with a Cy3 donor fluorophore at the s<sup>4</sup>U8 position within tRNA<sup>fMet</sup>) in the P site (Figure 6.3a) (Blanchard et al., 2004a). FRET generated between donor and acceptor fluorophores on the P site-bound fMet-(Cy3)tRNA<sup>fMet</sup> and incoming EF-Tu(GTP)Phe-(Cy5)tRNA<sup>Phe</sup> showed rapid progression from low to high FRET upon ternary complex binding to the ribosome, with the final FRET value of ~0.75 corresponding to full accommodation of Phe-(Cy5)tRNA<sup>Phe</sup> into the peptidyl-transferase center (Figures 6.3b and 6.3c). Dynamic fluctuations in the smFRET signal following accommodation were observed and attributed to tRNA dynamics after peptide bond formation (see Section IV).

The real-time evolution of smFRET observed during aa-tRNA selection contains a wealth of information concerning the conformational states through which the

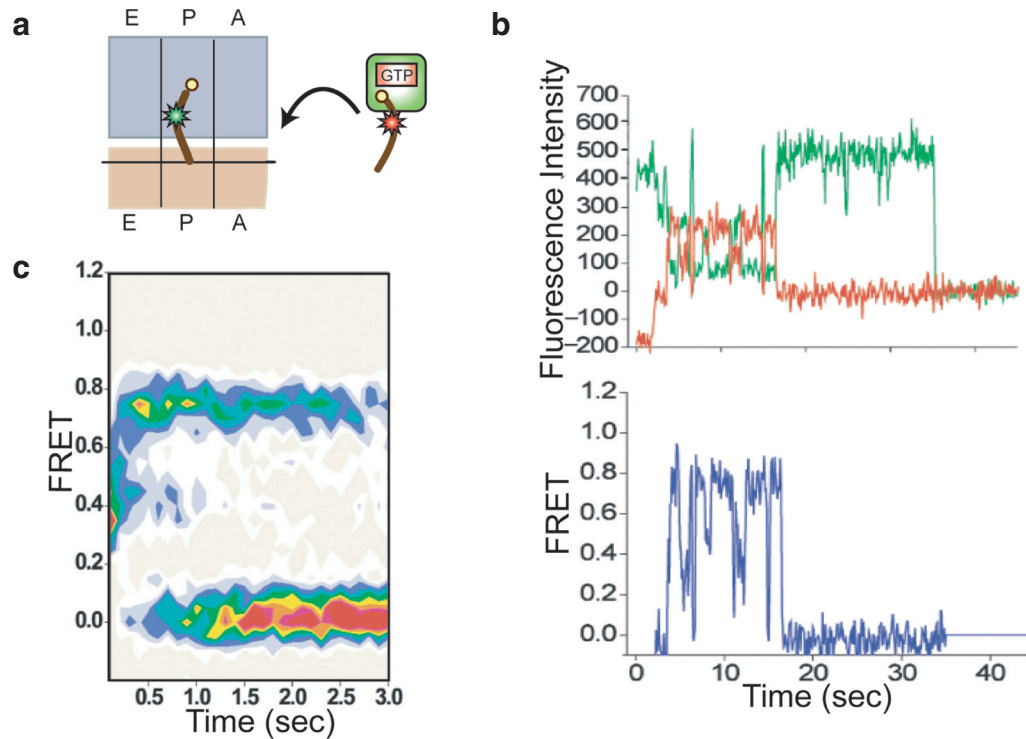


**FIGURE 6.3:** Selection of cognate aa-tRNA studied using tRNA-tRNA smFRET signal. (a) Cartoon representation of tRNA-tRNA smFRET signal. Cognate EF-Tu(GTP)Phe-(Cy5)tRNA<sup>Phe</sup> is delivered to a surface-immobilized initiation complex carrying fMet-(Cy3)tRNA<sup>fMet</sup>. (b) Sample Cy3 and Cy5 emission intensity versus time trajectories are shown in green and red, respectively (top). The corresponding smFRET versus time trajectory,  $FRET = I_{Cy5}/(I_{Cy3} + I_{Cy5})$ , is shown in blue (bottom). (c) Contour plot of the time evolution of population FRET, generated by superimposing the individual smFRET versus time traces and post-synchronizing to the first observation of  $FRET \geq 0.25$ . Contours are plotted from tan (lowest population) to red (highest population). Molecules in the  $\sim 0$ -FRET state arise from photobleaching, blinking of Cy5, and dissociation of tRNA from the ribosome. Figure adapted from Blanchard et al. (2004a), copyright © 2004 Nature Publishing Group, with permission from Macmillan Publishers Ltd.

aa-tRNA transits as it is selected by the ribosome; structural parameters (i.e., the relative distance between P- and A-site tRNAs) as well as kinetic parameters (i.e., the transition rates between different states) can be extracted from the smFRET versus time trajectories. Assignment of intermediate FRET states to particular conformational states was facilitated through the use of small-molecule inhibitors of protein synthesis that stall the aa-tRNA selection process at particular steps, and by programming the 30S subunit's A site with a near-cognate codon. In the presence of the antibiotic tetracycline or a near-cognate A-site codon, transient sampling of a low ( $\sim 0.35$ ) FRET state was observed, which was identified as the codon recognition state in which the codon-anticodon interaction is formed in the 30S subunit's decoding center (Figures 6.4a and 6.4b). The non-hydrolyzable GTP analog GDPNP and the antibiotic kirromycin were used to stall the ternary complex immediately before and after GTP hydrolysis, respectively, generating a mid- ( $\sim 0.5$ ) FRET state where EF-Tu is docked at the 50S subunit's GTPase-associated center (referred to hereafter simply as the GTPase

center) (Figures 6.4c and 6.4d). The transition from low to mid FRET, therefore, represents GTPase activation of EF-Tu. At this stage, aa-tRNA adopts the A/T configuration, first characterized structurally by chemical probing (Moazed and Noller, 1989a) and later by cryo-EM (see Chapter 7). Finally, the high- ( $\sim 0.75$ ) FRET state, achieved during uninhibited delivery of cognate EF-Tu(GTP)Phe-(Cy5)tRNA<sup>Phe</sup>, corresponds to successful accommodation of Phe-(Cy5)tRNA<sup>Phe</sup> into the peptidyl transferase center and peptide bond formation (Figure 6.3).

The low-FRET codon recognition state was found to represent a critical branchpoint in the mechanism used to preferentially select cognate over near-cognate aa-tRNAs. smFRET allowed direct observation of this intermediate – which had not been resolved in bulk biochemical experiments or in structural studies due to its transient nature – and permitted real-time observation of the frequencies and rates with which it is traversed by cognate versus near-cognate aa-tRNAs. When the 30S subunit's A site was programmed with the cognate UUU codon, the majority of EF-Tu(GTP)Phe-(Cy5)tRNA<sup>Phe</sup> progressed rapidly

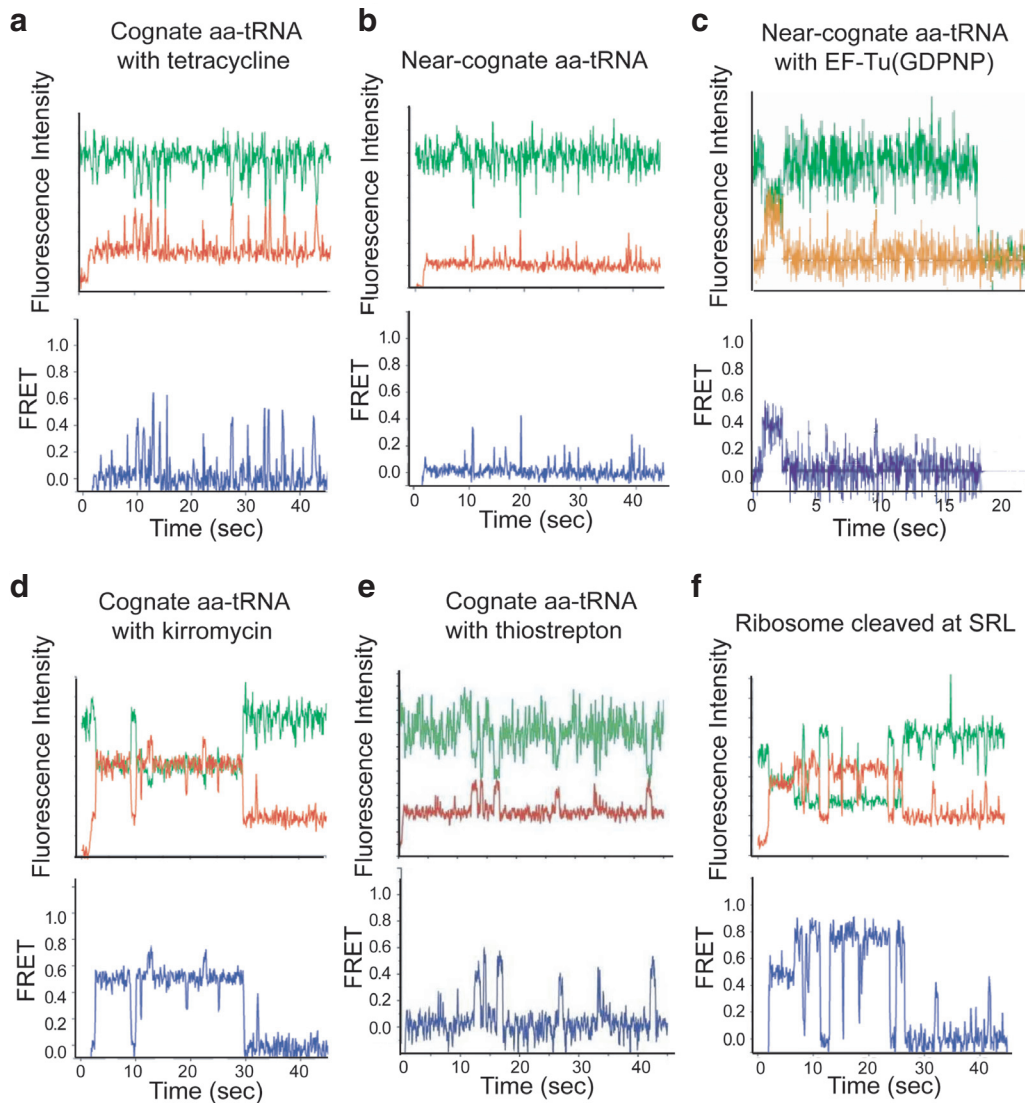


**FIGURE 6.4:** Single-molecule fluorescence intensities and smFRET versus time trajectories for aa-tRNA selection under various conditions. *Phe*-(*Cy5*)tRNA<sup>*Phe*</sup> (in ternary complex with EF-Tu and GTP or GDPNP) was stopped-flow delivered to ribosomal initiation complexes carrying *fMet*-(*Cy3*)tRNA<sup>*fMet*</sup> at the P site. *Cy3* and *Cy5* emission intensity versus time trajectories are shown in green and red, respectively (top). The corresponding smFRET versus time trajectories,  $FRET = I_{Cy5}/(I_{Cy3} + I_{Cy5})$ , are shown in blue (bottom). (a) Stopped-flow delivery of cognate ternary complex in the presence of 100  $\mu$ M tetracycline. (b) Stopped-flow delivery of near-cognate ternary complex. (c) Stopped-flow delivery of near-cognate aa-tRNA as a ternary complex with EF-Tu(GDPNP). (d) Stopped-flow delivery of cognate ternary complex in the presence of 200  $\mu$ M kirromycin. (e) Stopped-flow delivery of cognate ternary complex in the presence of 50  $\mu$ M thiostrepton. (f) Stopped-flow delivery of cognate ternary complex to ribosomal complexes cleaved at the sarcin-ricin loop (SRL). Figures (a), (b), (d) and (f) are reproduced from Blanchard et al. (2004a), copyright © 2004 Nature Publishing Group, with permission from Macmillan Publishers Ltd., Figure (c) is reproduced from Lee et al. (2007), copyright © 2007 National Academy of Sciences, U.S.A., and Figure (e) is reproduced from Gonzalez et al. (2007), copyright © 2007 RNA Society.

through the codon recognition state (low FRET) en route to GTPase activation (mid FRET) and accommodation (high FRET) (Figure 6.3). In the presence of a near-cognate CUU codon, however, the majority of incoming ternary complexes are unable to progress past the codon recognition state, instead only transiently sampling this state

before dissociating from the ribosome (Figure 6.4b). For near-cognate ternary complexes, sampling of the low-FRET codon recognition state was followed by a transition to higher FRET values only 11% of the time, versus 65% of the time for cognate ternary complexes. Furthermore, analysis of rates exiting the codon recognition state

demonstrated that near-cognate ternary complexes have both a higher rate of dissociation compared with cognate ternary complexes ( $k_{\text{low} \rightarrow 0}$ ; 16.2  $\text{sec}^{-1}$  versus 6.4  $\text{sec}^{-1}$ , respectively) and also a slower rate of transit to the GTPase-activated state ( $k_{\text{low} \rightarrow \text{mid}}$ ; 2  $\text{sec}^{-1}$  versus 11.8  $\text{sec}^{-1}$ , respectively). These observations shed light on the induced-fit mechanism that acts to stabilize the binding of a cognate ternary complex and to accelerate its GTPase activation. Formation of the cognate codon-anticodon interaction specifically accelerates transit from the low- to the mid-FRET state. Therefore, the allosteric mechanism linking cognate codon-anticodon recognition in the decoding center to enhanced rates of GTPase activation by EF-Tu involves a movement of aa-tRNA toward the P site, allowing productive interactions to be made between the ternary complex and the 50S subunit's GTPase center that stimulate EF-Tu's GTP hydrolysis activity.

### III.3 Thermally Driven Fluctuations of the Ribosome-tRNA Complex Permit Sampling of Conformational States Along the aa-tRNA Selection Pathway

The kinetic barrier separating the low-FRET codon recognition state from the mid-FRET GTPase-activated state is overcome through large thermal fluctuations of the ternary complex-bound ribosomal complex. This feature of initial selection was highlighted by higher-time-resolution smFRET measurements of the delivery of EF-Tu(GDPNP)Phe-(Cy5)tRNA<sup>Phe</sup> to ribosomal initiation complexes carrying fMet-(Cy3)tRNA<sup>fMet</sup> in the P site (Lee et al., 2007). In the presence of GDPNP, both cognate and near-cognate aa-tRNAs were found to fluctuate reversibly between the low- and mid-FRET states, reporting on attempts by the ternary complex to form stabilizing contacts with the GTPase center of the 50S subunit (Figure 6.4c). Stabilization of a long-lived mid-FRET state was interpreted to correspond to successful docking of the ternary complex at the GTPase center, where all stabilizing contacts between the ribosome and ternary complex required for GTPase activation have been formed. Specifically, interactions of the ternary complex with ribosomal proteins L10, L7/L12, L11 and its associated 23S rRNA, and the sarcin-ricin loop of 23S rRNA presumably play important roles in this stabilization. Short-lived excursions of the ternary complex to mid FRET, with lifetimes less than 100 ms were also observed (Figure 6.4c). These were interpreted as unsuccessful attempts to dock at the GTPase center, in which only a subset of the requisite stabilizing interactions are formed; this short-lived mid-FRET state was termed the pseudo-GTPase-activated state. Both cognate and near-cognate aa-tRNAs fluctuate rapidly into and out of the pseudo-GTPase-activated state before successful stable binding to the GTPase center. However, detailed kinetic analysis revealed that cognate aa-tRNAs fluctuate to mid FRET more often than near-cognate

aa-tRNAs (27 attempts  $\text{s}^{-1}$  versus 8 attempts  $\text{s}^{-1}$ , respectively). Additionally, fluctuations to mid FRET were more likely to result in successful docking for cognate as compared with near-cognate aa-tRNA; on average, cognate aa-tRNAs underwent two attempts per every successful docking event, compared to four for near-cognate aa-tRNA. These findings imply that the induced-fit rearrangements of the ribosomal complex triggered by cognate codon-anticodon interactions position the cognate ternary complex in a favorable orientation, such that fluctuations to the GTPase-activated state can occur more readily and with a higher probability of success. These results, in addition to highlighting the role of thermal fluctuations in aa-tRNA selection, emphasized the dynamic and inherently reversible nature of kinetic steps in the early stages of the aa-tRNA selection pathway.

Dynamic fluctuations of the tRNA-tRNA smFRET signal, corresponding to transient sampling of conformational states in the aa-tRNA selection pathway, have also been observed for ternary complexes stalled at mid FRET before and after GTP hydrolysis using GDPNP and the antibiotic kirromycin, respectively (Blanchard et al., 2004a). Kirromycin binds directly to EF-Tu and permits GTPase activation and GTP hydrolysis but blocks the subsequent conformational change of EF-Tu to its GDP-bound form. In the presence of either GDPNP or kirromycin, residency at the mid-FRET state is interrupted by brief excursions to both the low- and high-FRET states (Figure 6.4d). This behavior hints at the ability of the aa-tRNA to sample relevant conformational states of the reaction pathway even in the absence of GTP hydrolysis or EF-Tu's conformational change. It is tempting to speculate, then, that EF-Tu and GTP hydrolysis may not be strictly required for incorporation of aa-tRNA into the ribosomal A site. Perhaps the requisite aa-tRNA-ribosome interactions can be made, and the relevant conformational states sampled, even without EF-Tu. In support of this notion, factor-free translation from a poly(U) template can occur in vitro, albeit at a much slower rate than in the presence of translation factors and GTP (Pestka, 1969; Gavrilova and Spirin, 1971). In this view, aa-tRNA selection by the primordial ribosome may have predated the evolution of translation factors, and EF-Tu may have evolved later to increase the speed, directionality, and fidelity of this process.

### III.4 Regulation of aa-tRNA Selection by Antibiotics, Ribosome Structural Elements, and Amino Acid-tRNA Pairing

As described in the previous sections, the tRNA-tRNA smFRET signal allows direct observation of aa-tRNA's stepwise movement through the various conformational states that comprise the aa-tRNA selection process. As such, it provides a powerful experimental framework for investigating the effects of ribosome-targeting antibiotics

that interfere with aa-tRNA selection. This approach has proved useful in identifying the particular stage at which antibiotics act, as well as the kinetic mechanism by which they interfere with protein synthesis. As already discussed, the antibiotic tetracycline, whose primary binding site is located near the 30S subunit's A site (Brodersen et al., 2000; Pioletti et al., 2001), was shown to block progression of the ternary complex from the low-FRET codon recognition state to the mid-FRET GTPase-activated state. Upon sampling of a cognate or near-cognate codon-anticodon interaction in the presence of tetracycline, ternary complexes dissociate rapidly from the ribosome (Figure 6.4a). In contrast, thiostrepton, a thiazole antibiotic that binds to ribosomal protein L11 and the associated rRNA helices H43 and H44 of the 50S subunit's GTPase center (Harms et al., 2008), exerts its inhibitory action at the mid-FRET state (Figure 6.4e) (Gonzalez et al., 2007). This drug does not affect progression of the EF-Tu(GTP)Phe-(Cy5)tRNA<sup>Phe</sup> ternary complex through the codon recognition state, but instead prevents stable binding of the ternary complex at the GTPase center, with an observed mid-FRET lifetime of ~26 ms. Therefore, thiostrepton likely acts by blocking stabilizing contacts between the ternary complex and the L11 protein and/or L11-associated rRNA. Consequently, the ternary complex is unable to progress past the mid-FRET state, instead being rejected from the GTPase center and retracing its steps back through the codon recognition state before dissociating from the ribosome.

Comparison of these results with smFRET data collected using ribosomes with a cleaved sarcin-ricin loop has aided in the assignment of specific functional roles to distinct structural components of the ribosome's GTPase center. The sarcin-ricin loop represents an important component of the GTPase center, which has been shown to interact with EF-Tu's guanine nucleotide-binding domain (Schmeing et al., 2009; Villa et al., 2009). Like binding of thiostrepton, cleavage of the sarcin-ricin loop blocks progression of the EF-Tu(GTP)Phe-(Cy5)tRNA<sup>Phe</sup> ternary complex past the mid-FRET state, but through an entirely different mechanism (Blanchard et al., 2004a). In the case of a cleaved sarcin-ricin loop, ternary complexes transit to the GTPase center but become trapped there (Figure 6.4f), with a lifetime of ~8–12 s, in contrast to the transient (~26 ms) excursions to the GTPase center observed in the presence of thiostrepton. A model thus emerges in which the L11 region mediates stable binding of the ternary complex to the GTPase center, whereas the sarcin-ricin loop stimulates EF-Tu's GTP hydrolysis activity (Gonzalez et al., 2007).

Another, recent application of the tRNA-tRNA smFRET signal has been to explore the role of amino acid identity and amino acid-tRNA pairing in the selection process (Efrim et al., 2009). Using a ribozyme capable of misacylating tRNAs with non-native amino acids, misacylated

Ala-tRNA<sup>Phe</sup> and Lys-tRNA<sup>Phe</sup> were prepared and shown to be efficiently selected by the ribosome, capable of participating in peptide bond formation to nearly the same extent as correctly charged Phe-tRNA<sup>Phe</sup> in a dipeptide formation assay. However, competition experiments in which ribosomal initiation complexes were presented with an equimolar mixture of correctly charged and misacylated tRNA<sup>Phe</sup> demonstrated that the ribosome is capable of discriminating between the two species, leading to a slight preferential selection of tRNA<sup>Phe</sup> charged with its native amino acid (Phe-tRNA<sup>Phe</sup> was selected 3.7- and 2.2-fold more efficiently than Ala-tRNA<sup>Phe</sup> and Lys-tRNA<sup>Phe</sup>, respectively). This indicated that during aa-tRNA selection, the ribosome is sensitive to not only the codon-anticodon pairing, but also to the amino acid's identity and/or the specific amino acid-tRNA pairing.

Experiments utilizing the tRNA-tRNA smFRET signal revealed the molecular basis of this subtle discrimination. Sub-population analysis led to the classification of smFRET trajectories into two categories: trajectories exhibiting productive binding events that result in accommodation and peptide bond formation, and trajectories in which multiple A site sampling events were observed, none of which lead to full accommodation of aa-tRNA during the observation period. An increase in the latter sub-population was observed for both Ala-(Cy5)tRNA<sup>Phe</sup> and Lys-(Cy5)tRNA<sup>Phe</sup> compared with Phe-(Cy5)tRNA<sup>Phe</sup> (this sub-population accounts for 52% and 44% of the trajectories, respectively, compared with 16% for Phe-(Cy5)tRNA<sup>Phe</sup>), which closely mirrored the 3.7- and 2.2-fold enhanced selection efficiency of Phe-tRNA<sup>Phe</sup> compared to the misacylated species in the biochemical competition experiments. Therefore, the increased frequency of unproductive A-site sampling events points to the ribosome's capacity to sense amino acid identity and/or amino acid-tRNA pairing at an early stage in the aa-tRNA selection process, thereby discriminating against certain incorrectly charged tRNAs. This application of the tRNA-tRNA smFRET signal provides an important starting point for mechanistic studies of the translational machinery's response to tRNAs charged with unnatural amino acids that are poorly incorporated into proteins. A more detailed mechanistic understanding of how the ribosome discriminates against unnatural amino acids could facilitate biomedically relevant protein-engineering applications by aiding in the design of unnatural amino acid-tRNA pairings and, ultimately, mutant ribosomes that yield increased incorporation efficiencies.

#### IV. MRNA-TRNA TRANSLOCATION

##### IV.1 Transit of mRNA and tRNAs Through the Ribosome

After accommodation of aa-tRNA into the A site, peptide bond formation occurs rapidly, thereby transferring

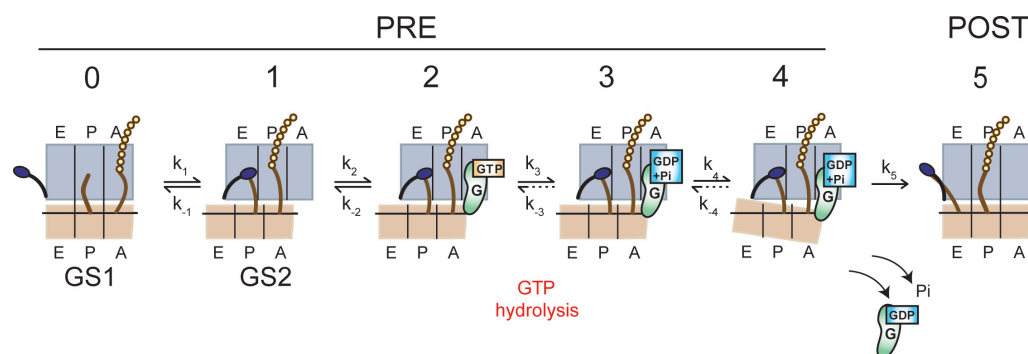


**FIGURE 6.5: Kinetic model for translocation.** Step 0→1: Following peptide bond formation, the PRE complex exists in a dynamic equilibrium between Global State 1 (GS1) and Global State 2 (GS2). Spontaneous conformational changes characterizing the GS1→GS2 transition include movement of the acceptor stems of A- and P-site tRNAs to the P and E sites on the 50S subunit, closing of the L1 stalk (dark blue), and a rotational movement of the 30S subunit relative to the 50S subunit. Step 1→2: Binding of EF-G(GTP) stabilizes GS2. Step 2→3: GTP hydrolysis by EF-G. Step 3→4: Further conformational rearrangements of the ribosome and EF-G that occur subsequent to GTP hydrolysis and facilitate translocation (Savelsbergh et al., 2003). Step 4→5: Translocation of mRNA and tRNAs on the 30S subunit and release of EF-G(GDP) and  $P_i$ . Adapted from Frank and Gonzalez (2010), copyright © 2010 Annual Reviews.

the nascent polypeptide to the A-site tRNA and deacylating the P-site tRNA. The resulting complex, referred to as the pretranslocation (PRE) complex, is the substrate for elongation factor G (EF-G)-catalyzed translocation of the mRNA-tRNA complex through the ribosome by precisely one codon. This translocation event moves A-site and P-site tRNAs into the P and E sites, respectively, and places the next mRNA codon into the decoding center so that it may be recognized by a new ternary complex in the next elongation cycle. The resulting ribosomal complex, bearing a peptidyl-tRNA in the P site and an empty A site, is referred to as a post-translocation (POST) complex (see Figure 6.5, which summarizes the kinetic steps of the translocation process). Conformational dynamics within the PRE and POST complexes has been the subject of intensive investigation by smFRET, and the results from these studies have enhanced our understanding of the mechanism and regulation of translocation. In particular, detailed smFRET investigations of conformational rearrangements of the PRE complex have provided direct evidence that translation factors and antibiotics are able to accelerate or impede translocation through specific modulation of the ribosome's dynamic conformational equilibria.

## IV.2 Conformational Rearrangements of the Pretranslocation Complex Required for Translocation

Large-scale conformational rearrangements of PRE complexes were initially identified through biochemical, ensemble FRET, and cryo-EM structural studies. Chemical probing experiments led to the discovery – subsequently corroborated by ensemble FRET measurements – that upon peptide bond formation, tRNAs spontaneously transition into intermediate “hybrid” configurations on the

ribosome, in which the 3'-terminal acceptor ends of the A- and P-site tRNAs occupy the large subunit P and E sites, respectively, while their anticodon stem loops remain bound at the small subunit A and P sites (termed A/P and P/E hybrid states, respectively) (Moazed and Noller, 1989b; Odom et al., 1990). Subsequent movement of the tRNA anticodon stems with respect to the 30S subunit, coupled with movement of the associated mRNA, is catalyzed by EF-G(GTP).

Cryo-EM reconstructions of PRE complex analogs containing vacant A sites (PRE<sup>-A</sup> complexes) and stabilized through the binding of EF-G(GDPNP) allowed visualization of the P-site tRNA bound in the P/E hybrid configuration and led to the discovery of additional large-scale conformational rearrangements of the PRE complex possibly associated with hybrid state formation (Frank and Agrawal, 2000; Valle et al., 2003). Comparison of cryo-EM reconstructions of PRE<sup>-A</sup> complexes in the presence and absence of EF-G(GDPNP) revealed three major conformational changes, highlighted in Figure 6.6. These were: (1) the aforementioned movement of deacylated P-site tRNA from the classical P/P to the hybrid P/E binding configuration; (2) movement of the universally conserved L1 stalk domain of the 50S E site ~20 Å toward the inter-subunit space, thereby establishing an intermolecular interaction with the elbow of the P/E tRNA; and (3) a counter-clockwise ratchet-like rotation of the 30S subunit with respect to the 50S subunit (when viewed from the solvent side of the 30S subunit). The global conformational states of the PRE<sup>-A</sup> complex observed by cryo-EM in the absence and presence of EF-G(GDPNP) will be referred to here as Global State 1 (GS1) and Global State 2 (GS2), respectively (Fei et al., 2008); we note that the analogous terms Macrostate I (MSI) and Macrostate II

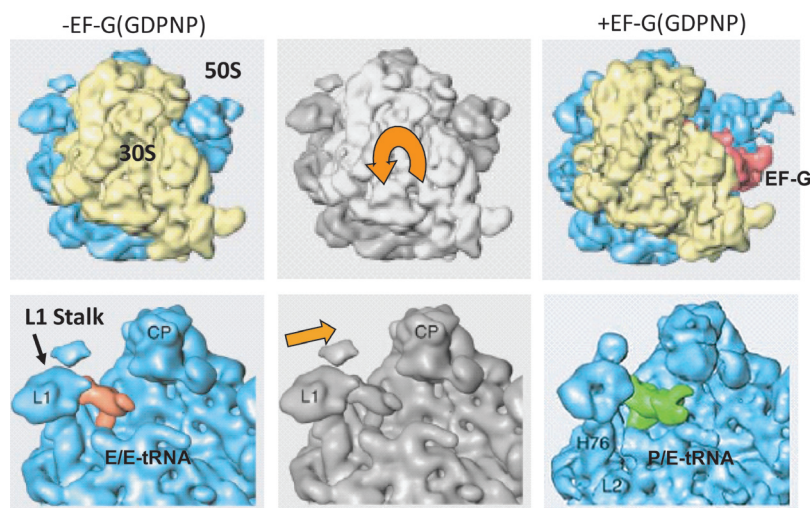


**FIGURE 6.6: Conformational rearrangements within the PRE complex inferred from cryo-EM reconstructions.** Images of the PRE complex analog ( $PRE^{-A}$ ) in the absence (left panel) and in the presence (right panel) of EF-G(GDPNP) reveal conformational rearrangements (middle panel), which include transition of the P-site tRNA from the classical to the hybrid binding configuration, counter-clockwise rotation of the 30S subunit relative to the 50S subunit (middle panel, top), and closing of the L1 stalk (middle panel, bottom). Adapted from Valle et al. (2003), copyright © 2003 Cell Press, with permission from Elsevier.

(MSII) are also in frequent use throughout the literature (Frank et al., 2007). The conformational changes characterizing the GS1→GS2 transition likely play a major role in facilitating the translocation reaction. Indeed, biochemical evidence lends support to the notion that GS2 represents an authentic on-pathway translocation intermediate (Dorner et al., 2006; Horan and Noller, 2007). It had been suggested early on that large-scale conformational rearrangements of PRE complexes – in particular a relative movement of the subunits, inferred from the ribosome’s universally conserved two-subunit architecture (Bretscher, 1968; Spirin, 1968) – underlie the translocation of mRNA and tRNAs through the ribosome, and the cryo-EM data provided important validation of this idea.

### IV.3 Spontaneous and Reversible Conformational Fluctuations of the Pretranslocation Complex are Thermally Driven

Numerous fluorophore-labeling strategies have been designed to investigate the conformational changes of PRE and  $PRE^{-A}$  complexes by smFRET, a subset of which will be discussed here (Figure 6.7). smFRET between elbow-labeled A- and P-site tRNAs was shown early on to report on the occupancy of the classical ( $\sim 0.74$  FRET) or hybrid ( $\sim 0.45$  FRET) states (Blanchard et al., 2004b). L1 stalk movement from an open to a closed conformation has been tracked through smFRET between fluorophores attached to ribosomal proteins L1 and L9 (Fei et al., 2009) (an L1-L33 smFRET signal has also been used for this

purpose in an independent study [Cornish et al., 2009]). Based on cryo-EM reconstructions of the L1 stalk in the open and closed states, an L1-L9 smFRET state centered at  $\sim 0.56$  FRET was assigned to the open L1 stalk conformation, while a second state centered at  $\sim 0.34$  FRET was assigned to the closed conformation. In the closed conformation, the L1 stalk can form inter-molecular contacts with the elbow region of P/E hybrid tRNA; smFRET signals between fluorophore-labeled L1 and P-site tRNA were developed to report on the formation (high FRET,  $\sim 0.84$ ) and disruption (low FRET,  $\sim 0.21$ ) of these contacts (Fei et al., 2008; Munro et al., 2009a). Finally, inter-subunit rotation has been monitored through smFRET between dye-labeled ribosomal proteins reconstituted with an S6(Cy5)-L9(Cy3) construct will be described below, in which smFRET states centered at  $\sim 0.56$  and  $\sim 0.4$  FRET were assigned to the non-rotated and rotated conformations, respectively (Ermolenko et al., 2007a; Cornish et al., 2008).

PRE and  $PRE^{-A}$  complexes are prepared via peptidyl transfer from the P-site tRNA to either aa-tRNA or the antibiotic puromycin at the A site, respectively (Fei et al., 2008; Munro et al., 2009a)). Puromycin mimics the 3'-terminal acceptor stem of aa-tRNA, participating in peptide bond formation to deacylate the P-site tRNA before dissociating from the ribosome (Traut and Monro, 1964). Steady-state smFRET measurements of PRE and  $PRE^{-A}$  complexes using the previously described donor-acceptor labeling schemes yield the striking observation of

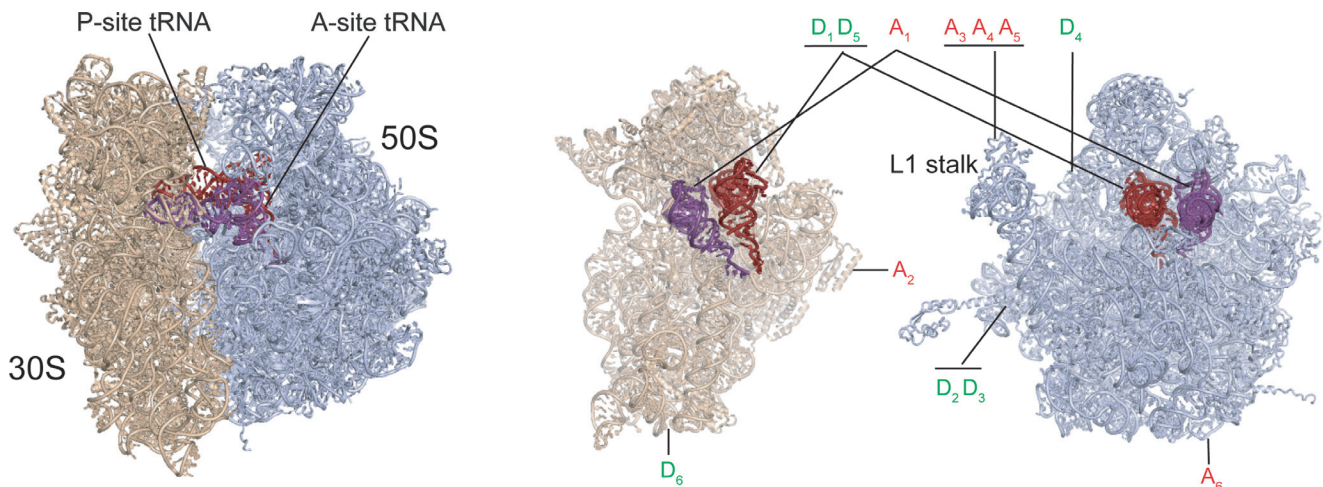


**FIGURE 6.7:** Positions of the translational machinery labeled with donor (D)/acceptor (A) fluorophore pairs in smFRET studies of translocation. The 70S ribosome (PDB ID: 2J00 and 2J01) carrying A- and P-site tRNAs (in purple and red, respectively) (left panel) is split into 30S and 50S subunits (in tan and lavender, respectively), which are viewed from the inter-subunit space (right panel).  $D_1$ :  $s^4U8$  of P-site tRNA<sup>Met</sup>;  $A_1$ :  $acp^3U47$  of A-site tRNA<sup>Phe</sup>.  $D_2$ : position 11 within N11C single-cysteine mutant of r-protein L9;  $A_2$ : position 41 within D41C single-cysteine mutant of r-protein S6.  $D_3$ : position 18 within Q18C single-cysteine mutant of r-protein L9;  $A_3$ : position 202 within T202C single-cysteine mutant of r-protein L1.  $D_4$ : position 29 within T29C single-cysteine mutant of r-protein L33;  $A_4$ : position 88 within A88C single-cysteine mutant of r-protein L1.  $D_5$ :  $acp^3U47$  of P-site tRNA<sup>Phe</sup>;  $A_5$ : position 202 within T202C single-cysteine mutant of r-protein L1, or position 55 within S55C single-cysteine mutant of L1.  $D_6$ : helix 44 of 16S rRNA (nucleotides 1450-1453);  $A_6$ : Helix 101 of 23S rRNA (nucleotides 2853-2864). Figure adapted from Frank and Gonzalez (2010).

spontaneous and stochastic conformational fluctuations, corresponding to dynamic and reversible exchange between classical and hybrid configurations of the tRNAs, open and closed conformations of the L1 stalk, formation and disruption of L1-tRNA interactions, and rotated and non-rotated inter-subunit orientations (Figure 6.8). These large-scale conformational rearrangements, which require extensive remodeling of RNA-RNA, protein-protein, and RNA-protein interactions, are observed to occur spontaneously, driven solely by thermal energy.

Each smFRET signal is consistent with a specific conformational change associated with the GS1→GS2 transition characterized by cryo-EM; taken together, the smFRET signals, therefore, imply spontaneous fluctuations of the entire PRE complex between the GS1 and GS2 conformational states. These results suggest that transition to GS2 – and thus forward progression along the translocation reaction coordinate – can occur in the absence of EF-G and GTP hydrolysis. Indeed, full rounds of spontaneous translocation have been observed *in vitro* in a factor-free environment, in which the ribosome moves slowly but directionally along the mRNA template to generate polypeptides of defined length (Gavrilova et al., 1976). It seems, therefore, that many, if not all, of the conformational rearrangements required for translocation can be accessed with the input of thermal energy alone. Fluctuations of the PRE complex observed by smFRET represent dynamic events likely important for promoting mRNA and tRNA movement during translocation; these

fluctuations may thus increase the probability that spontaneous translocation will occur.

Conformational fluctuations within the PRE complex appear to be triggered by deacylation of the P-site peptidyl-tRNA, an “unlocking” event that prepares the ribosome for movement of the mRNA-tRNA complex by one codon (Valle et al., 2003). Following translocation, the ribosome is converted back to a “locked” state in which large-scale dynamics appear to be largely suppressed (with the exception of L1 stalk dynamics, which are important for E-site tRNA release and will be discussed in depth in Section IV.6). This suppression of conformational dynamics is evident from smFRET interrogation of POST complexes containing a peptidyl-tRNA at the P site. Structural features characteristic of GS1 appear to predominate in POST complexes, with a large majority of ribosomes observed to be fixed in a non-rotated state with a strong preference for the classical tRNA configuration (Ermolenko et al., 2007a; Cornish et al., 2008).

Multiple cycles of ribosome locking and unlocking during translation elongation have been observed using an inter-subunit smFRET signal consisting of fluorescently labeled oligonucleotides hybridized to helical extensions engineered into h44 of 16S rRNA within the 30S subunit and H101 of 23S rRNA within the 50S subunit (Figure 6.7) (Marshall et al., 2008; Aitken and Puglisi, 2010). Using the H101(Cy5)-h44(Cy3) labeling scheme, peptide bond formation and ribosome unlocking are signaled by a high→low FRET transition, whereas



thus act to preserve the correct reading frame following translocation. Additionally, the locked conformation may facilitate selection of the next aa-tRNA and its precise positioning in the peptidyl transferase center. Following peptide bond formation, the POST complex is unlocked and converted to a dynamic PRE complex in which thermal fluctuations power conformational rearrangements that are required for translocation.

#### IV.4 Conformational Dynamics within Pretranslocation Complexes are Modulated by Magnesium Ion Concentration, tRNA Identity and Acylation State, and Antibiotics

Single-molecule FRET versus time trajectories that report on conformational fluctuations of the PRE complex contain a wealth of mechanistic information, allowing determination of the number of states sampled, their equilibrium population distributions ( $K_{eq}$ ), and the transition rates between states (i.e.,  $k_{state(i) \rightarrow state(j)}$ ). This information, which would be masked in bulk measurements due to the stochastic and asynchronous nature of the conformational fluctuations, is uniquely accessible to single-molecule techniques. Both the equilibrium distribution of states and the transition rates between states for the various conformational equilibria characterizing GS1  $\rightleftharpoons$  GS2 transitions were found to be highly sensitive to experimental conditions, including the concentration of  $Mg^{2+}$  ions, the absence, presence, identity, and acylation state of the tRNA ligands, the absence or presence of translation factors, and the absence or presence of ribosome-targeting antibiotics. Assuming that conformational changes associated with the GS1  $\rightarrow$  GS2 transition are a fundamental part of the translocation process, these observations suggest that specific control over ribosome dynamics within the PRE complex, through the acceleration/deceleration of conformational change and the stabilization/destabilization of specific conformational states, could provide an effective means for regulating the rate of translocation. In this view, ribosomal ligands may function by promoting or inhibiting conformational dynamics that are intrinsic to the ribosomal complex. Indeed, as described in the following paragraphs, the effect of changes in experimental conditions on the rate of translocation is often correlated with the effect of those changes on PRE complex dynamics.

The dynamic exchange of tRNAs between classical and hybrid configurations necessarily requires the disruption and formation of multiple tRNA-rRNA and tRNA-ribosomal protein interactions; this suggests that the classical  $\rightleftharpoons$  hybrid tRNA equilibrium may be modulated by the concentration of  $Mg^{2+}$  ions in solution because  $Mg^{2+}$  is known to play a crucial role in the folding and stabilization of RNA structures (Draper, 2004). Examination of the classical  $\rightleftharpoons$  hybrid tRNA equilibrium over a range of  $Mg^{2+}$  concentrations (3.5 to 15 mM) within a PRE complex

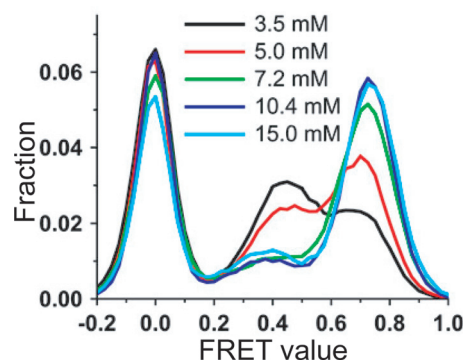


**FIGURE 6.10:**  $Mg^{2+}$ -dependence of tRNA classical  $\rightleftharpoons$  hybrid dynamic equilibrium tRNA dynamics were observed using the  $D_1/A_1$  smFRET probes shown in Figure 6.7. The distribution of FRET values is plotted as a function of  $Mg^{2+}$  concentration. FRET states centered at  $\sim 0.4$  and  $\sim 0.75$  FRET correspond to hybrid and classical tRNA configurations, respectively. The FRET state at  $\sim 0$  FRET arises from Cy5 blinking and photobleaching. Reproduced from Kim et al. (2007), copyright © 2007 Cell Press, with permission from Elsevier.

carrying N-acetyl-Phe(Cy5)tRNA<sup>Phe</sup> at the A site and deacylated (Cy3)tRNA<sup>Met</sup> at the P site revealed a  $Mg^{2+}$ -dependent shift in the equilibrium distribution of classical and hybrid configurations (Kim et al., 2007). Specifically, at low concentrations (3.5 mM) the hybrid configuration is favored. However, the equilibrium fraction of the classical configuration increases with increasing concentration of  $Mg^{2+}$ , with the classical and hybrid configurations becoming equally populated at  $\sim 4$  mM  $Mg^{2+}$  (Figure 6.10). Lifetime analysis revealed that this shift occurs primarily through a  $Mg^{2+}$ -dependent stabilization of the classical configuration, whose lifetime increases as a function of  $Mg^{2+}$ , whereas the lifetime of the hybrid configuration is unaffected. In structural terms, this is interpreted to mean that classically bound tRNAs form a more extensive and compact network of  $Mg^{2+}$ -stabilized tRNA-rRNA and/or tRNA-ribosomal protein interactions. At high  $Mg^{2+}$  concentrations ( $\sim 7$  mM and above), the classical configuration is almost exclusively favored on account of a decreased rate of classical  $\rightarrow$  hybrid transitions. These results offer a mechanistic explanation for the known inhibitory and stimulatory effects, respectively, of high and low  $Mg^{2+}$  concentration on the rate of translocation. At very high  $Mg^{2+}$  concentrations ( $\sim 30$  mM), translocation is blocked almost entirely, even in the presence of EF-G(GTP) (Spirin, 1985), which can be rationalized by a  $Mg^{2+}$ -induced stalling of the classical  $\rightarrow$  hybrid tRNA transition evidenced by smFRET. At the other extreme of low  $Mg^{2+}$  ( $\sim 3$  mM), spontaneous translocation can proceed rapidly (Spirin, 1985), an effect presumably linked to the accelerated rate of the classical  $\rightarrow$  hybrid transition under low- $Mg^{2+}$  conditions. Thus, smFRET evidence suggests that the rate of the classical  $\rightarrow$  hybrid tRNA transition is closely linked with the rate of translocation, implying that

under certain conditions, movement of tRNAs into their hybrid configuration may represent a rate-limiting step for translocation of mRNA and tRNAs through the ribosome.

Changes in the acylation state and identity of the P- and A-site tRNAs within PRE complexes have similarly been found to influence the energetics of its conformational fluctuations. As discussed earlier, the presence of a peptide on the P-site tRNA (i.e., in a POST complex) correlates with a locked ribosome in which ribosome and tRNA dynamics are suppressed, whereas ribosomes bearing a deacylated P-site tRNA (i.e., in a PRE complex) are unlocked and exhibit pronounced dynamic behavior. In addition, ribosome dynamics have been shown to be sensitive to the identity of the P-site tRNA. For example, a comparison of inter-subunit rotation dynamics within four different PRE<sup>-A</sup> complexes differing only in the identity of the deacylated P-site tRNA (tRNA<sup>Met</sup>, tRNA<sup>Phe</sup>, tRNA<sup>Tyr</sup>, and tRNA<sup>Met</sup> were used) revealed distinct thermodynamic and kinetic parameters underlying reversible inter-subunit rotation (Cornish et al., 2008). Different P-site tRNA species, therefore, make sufficiently unique contacts with the ribosome to influence large-scale structural rearrangements at the subunit interface in a characteristic way.

Similarly, the presence and acylation state of the A-site tRNA appears to dictate thermodynamic and kinetic behavior of conformational equilibria monitored by the individual smFRET signals. For example, the presence of A-site dipeptidyl-tRNA versus aa-tRNA increases the population of the hybrid configuration by increasing the rate of classical→hybrid tRNA transitions, as monitored by the tRNA-tRNA smFRET signal (Blanchard et al., 2004b). Likewise, using the L1-tRNA smFRET signal, addition of aa-tRNA to PRE complexes caused a slight increase in the rate with which the L1 stalk-P/E tRNA interaction is formed, with minimal effect on the rate with which this interaction is disrupted. Occupancy of the A site by a peptidyl-tRNA increased the forward rate by an additional six-fold, again with minimal effect on the reverse rate (Fei et al., 2008). Finally, the presence of a peptidyl-tRNA at the A site of PRE complexes shifts the equilibrium from the open to the closed L1 stalk conformation, as monitored by the L1-L9 smFRET signal, primarily by accelerating the rate of open→closed L1 stalk transitions (Fei et al., 2009).

From the data discussed in the previous paragraphs, a picture begins to emerge in which large-scale conformational rearrangements of the entire PRE complex can be allosterically controlled through even subtle and highly localized changes in interactions between the ribosome and its ligands (i.e., the presence of peptidyl- versus aa-tRNA at the A site). This feature of the PRE complex has been exploited by ribosome-targeting antibiotics, which, as described in Section III for drugs that inhibit aa-tRNA selection, often function by inhibiting the dynamics of

the translational machinery. Indeed, smFRET studies have provided evidence that translocation inhibitors specifically interfere with the conformational dynamics of PRE complexes. One example is the potent translocation inhibitor viomycin, which binds at the interface of the 30S and 50S subunits between helix 44 within the 16S rRNA and helix 69 within the 23S rRNA (Yamada et al., 1978; Stanley et al., 2010). Viomycin halts inter-subunit rotation dynamics and causes a net stabilization of the rotated state (Ermolenko et al., 2007b; Cornish et al., 2008). In addition, viomycin has been shown to slow classical⇌hybrid tRNA fluctuations (Kim et al., 2007; Feldman et al., 2010), although there are conflicting reports regarding the question of whether the drug stabilizes the classical or the hybrid configuration (Ermolenko et al., 2007b; Kim et al., 2007; Feldman et al., 2010).

smFRET investigations of PRE complexes were also conducted in the presence of a collection of aminoglycoside antibiotics (Feldman et al., 2010), drugs that bind to helix 44 within the 16S rRNA, stabilizing a conformation of the universally conserved 16S rRNA nucleotides A1492 and A1493 in which they are displaced from helix 44, adopting extrahelical positions that allow them to interact directly with the codon-anticodon helix at the decoding center (Carter et al., 2000). The aminoglycosides were shown to suppress tRNA dynamics, in general decreasing the rate of transition out of the classical tRNA binding configuration and causing a net stabilization of the classical state. The magnitude of these effects elicited by each of the aminoglycosides tested, although modest, correlated with the reduction in translocation rate observed in the presence of each drug (results from kanamycin, gentamycin, paromomycin, and neomycin are shown in Figure 6.11) (Feldman et al., 2010). Therefore, stabilization of the classical state and inhibition of transitions into the hybrid state represents a general mechanism for translocation inhibition by aminoglycosides, with subtle differences in antibiotic chemical structure dictating the degree of inhibition. Taken together, the results presented in this section illustrate that inhibition of ribosome and/or tRNA dynamics within the PRE complex represents a general inhibition strategy leveraged by a variety of ribosome-targeting antibiotics.

#### IV.5 Regulation of Pretranslocation Complex Dynamics by EF-G

Perhaps the most dramatic effect on ribosome dynamics within the PRE complex is elicited by EF-G, the elongation factor responsible for catalysis of full mRNA-tRNA translocation. smFRET analysis revealed that binding of EF-G(GDPNP) to PRE<sup>-A</sup> complexes leads to stabilization of all conformational features characterizing the GS2 ribosome: ribosomal subunits are stabilized in their rotated conformation, the L1 stalk strongly favors the closed conformation, and the P-site tRNA is stabilized in the P/E

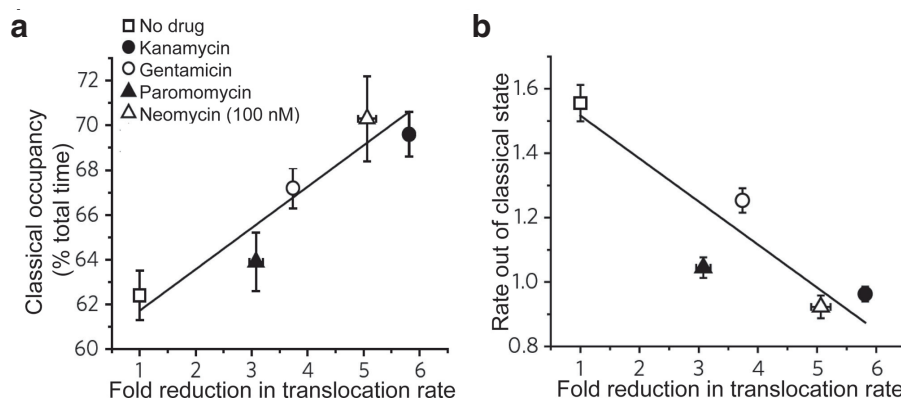


**FIGURE 6.11: Stabilization of the classical state is strongly correlated with inhibition of translocation by decoding site-binding aminoglycosides. (a) A strong correlation is observed between time-averaged classical state occupancy and fold-reduction of the single-step translocation rate of wild-type ribosomes in the presence of drug (20  $\mu$ M, unless otherwise noted). (b) A strong correlation is also observed between translocation rates and the rate constant of transitioning from the classical to hybrid states. Reproduced from Feldman et al. (2010), copyright © 2010 Nature Publishing Group, with permission from Macmillan Publishers Ltd.**

hybrid state where it forms a long-lived inter-molecular interaction with the L1 stalk (Ermolenko et al., 2007a; Cornish et al., 2008; Cornish et al., 2009; Fei et al., 2009). Particularly remarkable is the stabilization of the closed state of the L1 stalk, which demonstrates that binding of EF-G(GDPNP) to the ribosome's GTPase center can allosterically regulate L1 stalk dynamics  $\sim 175$  Å away at the ribosomal E site. A major role of EF-G, therefore, appears to be to bias intrinsic conformational fluctuations of the ribosome toward the on-pathway translocation intermediate GS2. In accord with the ability of the ribosome to translocate in the absence of translation factors (Pestka, 1969; Gavrilova et al., 1976; Bergemann and Nierhaus, 1983), one of EF-G's main mechanistic functions may be to stabilize GS2, preventing backward fluctuations along the translocation reaction coordinate and thus guiding the directionality of a process that the ribosome is inherently capable of coordinating on its own. This model finds strong support from biochemical experiments demonstrating that EF-G(GDPNP) stimulates the rate of translocation  $\sim 1,000$ -fold relative to uncatalyzed, spontaneous translocation, and that GTP hydrolysis in the EF-G(GTP)-catalyzed reaction provides an additional rate enhancement of only  $\sim 50$ -fold (Rodnina et al., 1997; Katunin et al., 2002). GTP hydrolysis, which, based on fast kinetics measurements, precedes movement of the mRNA-tRNA duplex on the small subunit, likely leads to conformational changes in EF-G and the ribosome that promote the second step of translocation (Rodnina et al., 1997; Taylor et al., 2007).

As previously discussed, a full round of mRNA-tRNA translocation converts the PRE complex into a POST complex in which non-rotated subunits and classical tRNA configurations characteristic of GS1 prevail and ribosome and tRNA dynamics are suppressed (Ermolenko et al., 2007a;

Cornish et al., 2008; Fei et al., 2008). This effect could be observed in real time through stopped-flow delivery of EF-G(GTP) to PRE complexes with the inter-subunit S6(Cy5)-L9(Cy3) smFRET pair (Cornish et al., 2008). The PRE complex exhibits rotated  $\rightleftharpoons$  non-rotated inter-subunit fluctuations until the delivery of EF-G(GTP), which binds to the PRE complex and catalyzes full translocation, thereby rectifying inter-subunit dynamics and locking the ribosome in the post-translocation, non-rotated state (Figure 6.12).

#### IV.6 Conformational Dynamics of the L1 Stalk Before, During, and After Translocation

In contrast to the predominately static behavior of the inter-subunit smFRET signal in POST complexes, the L1-L9 smFRET signal demonstrates a persistence of L1 stalk dynamics. The L1 stalk, as suggested by its conservation throughout all kingdoms of life (Nikulin et al., 2003), represents an important structural component of the ribosome that likely plays a crucial role in both the translocation event and subsequent release of deacylated tRNA from the E site (Valle et al., 2003; Andersen et al., 2006). Results from a study in which tRNA dynamics were probed using a tRNA-tRNA smFRET signal hint at the role of the L1 stalk in promoting translocation. In this study, stabilization of the classical tRNA configuration was observed in PRE complexes formed with L1-depleted mutant ribosomes, an effect that was correlated with the slowed rate of translocation observed in the absence of L1 (Subramanian and Dabbs, 1980; Munro et al., 2007). Further single-molecule evidence underscoring the functional importance of the L1 stalk was achieved by monitoring L1-tRNA interactions during real-time EF-G-catalyzed

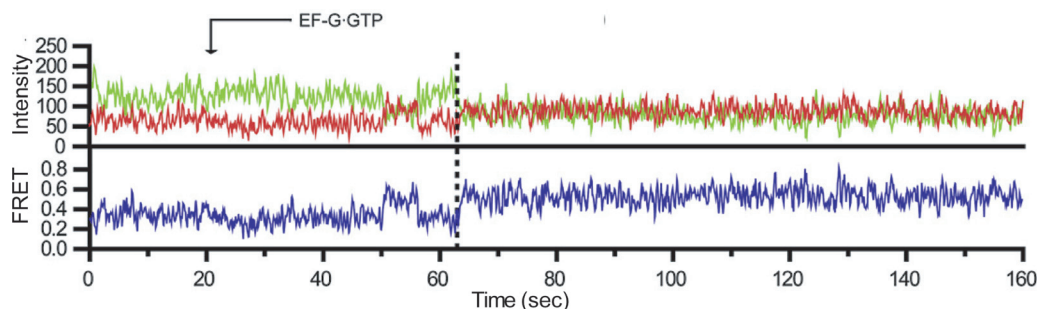


**FIGURE 6.12:** *EF-G(GTP)-catalyzed translocation rectifies inter-subunit rotation dynamics and converts the ribosome into the non-rotated state. The  $D_2/A_2$  smFRET probes shown in Figure 6.7 were used to report on inter-subunit rotation. EF-G(GTP) (300 nM EF-G, 250  $\mu$ M GTP) was added at  $\sim 20$  s (arrow) to PRE complexes containing deacylated tRNA<sup>Met</sup> bound to the P site and N-Ac-Phe-tRNA<sup>Phe</sup> bound to the A site. Translocation is observed as the transition to the stable high-FRET state (vertical dashed line). Reproduced from Cornish et al. (2008), copyright © 2008 Cell Press, with permission from Elsevier.*

translocation reactions (Fei et al., 2008). Stopped-flow delivery of Lys-tRNA<sup>Lys</sup> and EF-G(GTP) to a POST complex bearing L1(Cy5) and fMet-Phe-(Cy3)tRNA<sup>Phe</sup> in the P site leads to peptidyl transfer followed by EF-G(GTP)-catalyzed translocation. The smFRET versus time trajectories exhibit a sharp transition from low to high FRET upon peptidyl transfer (corresponding to the formation of inter-molecular contacts between L1 and the tRNA's elbow region), followed by stable occupancy of the high-FRET state until fluorophore photobleaching (Figure 6.13b). This is in contrast to the analogous experiment performed in the

absence of EF-G(GTP), where the initial transition from low to high FRET is followed by fluctuations between the two FRET states (corresponding to repetitive formation and disruption of L1-tRNA contacts) (Figure 6.13a). These results suggest that during EF-G(GTP)-catalyzed translocation, inter-molecular interactions formed between the L1 stalk and P/E-tRNA are maintained during the movement of the deacylated tRNA from the hybrid P/E configuration into the classical E/E configuration. Formation and maintenance of these interactions provides a molecular rationale to help explain how the L1 stalk

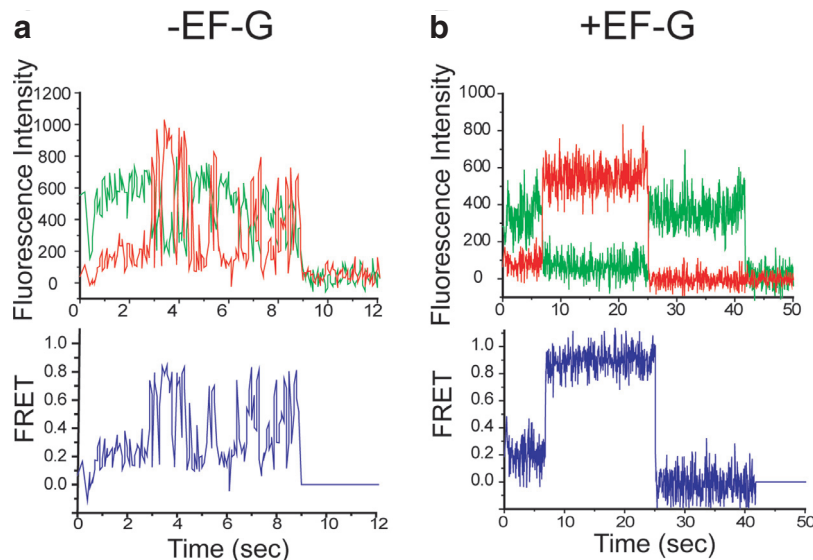


**FIGURE 6.13:** *Real-time measurement of L1 stalk-tRNA interaction during a full elongation cycle. The  $D_5/A_5$  smFRET probes shown in Figure 6.7 were used to study the L1 stalk-tRNA interaction. Stopped-flow delivery of 100 nM EF-Tu(GTP)Lys-tRNA<sup>Lys</sup> in the absence (a) and presence (b) of 1  $\mu$ M EF-G(GTP) to surface-immobilized POST complexes bearing L1(Cy5) and fMet-Phe-(Cy3)tRNA<sup>Phe</sup> at the P site. Reproduced from Fei et al. (2008), copyright © 2008 Cell Press, with permission from Elsevier.*

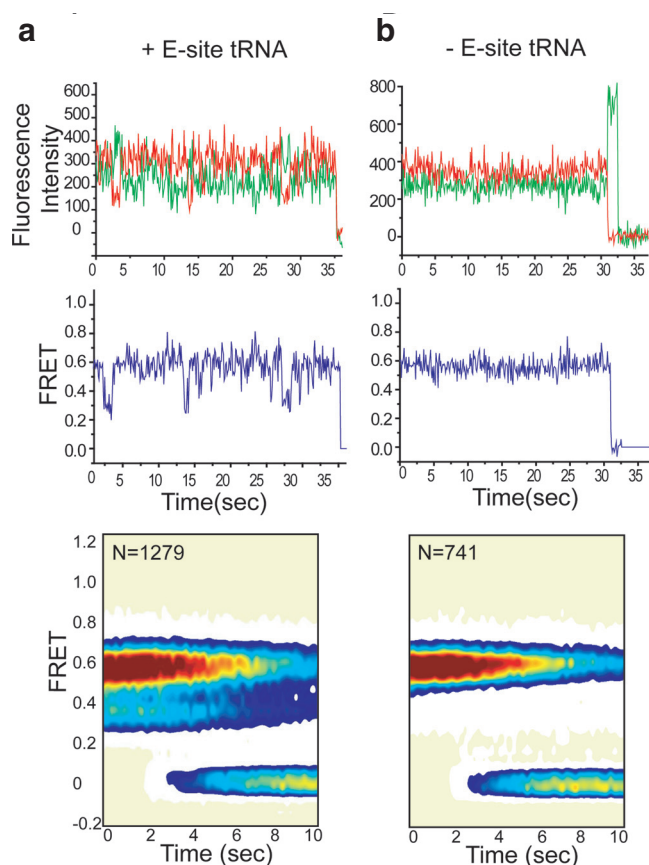


**FIGURE 6.14: L1 stalk conformational dynamics within POST complexes.** The intrinsic conformational dynamics of the L1 stalk within POST complexes were studied using the  $D_3/A_3$  smFRET probes shown in Figure 6.7. (a) In an authentic POST complex containing an E-site tRNA, the L1 stalk undergoes fluctuations between open ( $\sim 0.56$  FRET) and half-closed ( $\sim 0.34$  FRET) conformations. (b) In a POST complex with a vacant E site, the L1 stalk predominately occupies the open conformation. Reproduced from Fei et al. (2009), copyright © 2009 National Academy of Sciences, U.S.A.

facilitates the translocation reaction (Subramanian and Dabbs, 1980).

Following translocation, L1 stalk dynamics within the POST complex (in this case containing deacylated tRNA<sup>Phe</sup> at the E site and fMet-Phe-Lys-tRNA<sup>Lys</sup> at the P site) may actively promote the deacylated tRNA's dissociation from the ribosome. The majority of smFRET versus time trajectories collected using the L1-L9 smFRET signal with this POST complex exhibited fluctuations between low- and high-FRET states (Fei et al., 2009) (Figure 6.14a). The low-FRET state within POST complexes likely corresponds to a "half-closed" conformation of the L1 stalk identified by Cornish et al. (2009), whereas the high-FRET state reports on the open stalk conformation. The observed fluctuations likely originate from a sub-population of complexes whose E-site tRNA has not yet been released, because this dynamic sub-population largely disappears for POST complexes from which E-site tRNA was quantitatively

dissociated prior to smFRET measurements. For these POST complexes with a vacant E site, the majority of smFRET trajectories instead correspond to a stable open conformation of the L1 stalk (Figure 6.14b). In contrast to the dynamic fluctuations of the L1-L9 signal, the L1-tRNA signal yields a stable high-FRET value in the analogous POST complex (Figure 6.13b). This observation strongly suggests that inter-molecular interactions between L1 and the E-site tRNA are maintained while the stalk fluctuates between open and half-closed conformations, thus implying a reconfiguration of the tRNA between at least two different configurations within the E site. Analogous to the L1 stalk's role in directing translocation of tRNA from the P to the E site, it is likely that maintenance of L1-tRNA contacts during the tRNA's residency at the E site allows opening of the stalk to guide the release trajectory of deacylated tRNA from the POST complex. Interestingly, the rate of stalk opening was found to be  $\sim$ ten-fold faster than the rate of E-site tRNA release, implying that multiple fluctuations of the L1 stalk/E-site tRNA complex may occur prior to ejection. Therefore, opening of the L1 stalk, though presumably required for release of E-site tRNA from the POST complex, may not constitute the rate-limiting step for this process.

## V. BEYOND ELONGATION: SMFRET INVESTIGATIONS OF TRANSLATION INITIATION, TRANSLATION TERMINATION, AND RIBOSOME RECYCLING

### V.1 Translation Factor-Mediated Modulation of Ribosome Dynamics as a Unifying Theme During All Stages of Protein Synthesis

In Sections III and IV, we described how conformational dynamics of the ribosome and its tRNA substrates are modulated during the elongation phase of protein synthesis, providing a regulatory mechanism that is exploited by EF-Tu and EF-G to promote aa-tRNA selection and translocation, respectively, as well as by ribosome-targeting antibiotics that impede these processes. Although the majority of smFRET studies to date have focused on elongation, recent smFRET investigations into initiation, termination, and ribosome recycling have provided evidence that translation factors serve an analogous function at the beginning and end of each round of protein synthesis. Modulation of the ribosome's global architecture through factor-dependent shifts in the translational machinery's conformational equilibria may serve as a general paradigm for translation regulation throughout all stages of protein synthesis.

### V.2 Translation Initiation

During initiation of protein synthesis, a ribosomal initiation complex is assembled from its component parts in

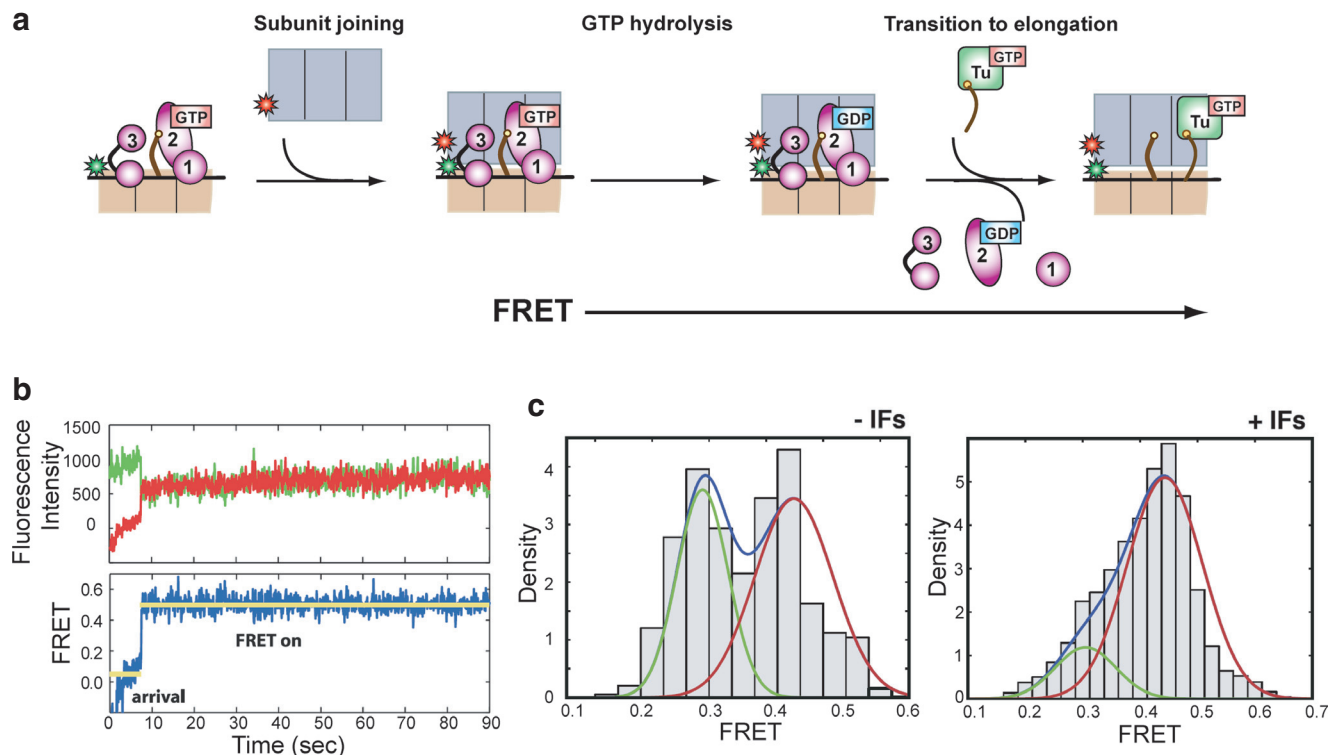


**FIGURE 6.15: Regulation of ribosomal conformational dynamics by initiation factors during translation initiation.** The  $D_6/A_6$  smFRET probes shown in Figure 6.7 were used to study the inter-subunit conformation of the ribosome during translation initiation. (a) Surface immobilization of Cy3-labeled 30S initiation complexes containing 30S subunits, initiation factors, fMet-tRNA<sup>fMet</sup>, and mRNA followed by delivery of Cy5-labeled 50S subunits results in formation of a 70S initiation complex and establishment of a FRET signal sensitive to inter-subunit conformation. (b) Representative Cy3/Cy5 emission intensities and smFRET versus time trace. Upon stopped-flow delivery of Cy5-50S, an initial dwell time is observed followed by a burst of FRET. The FRET signal is stable, with the observation time often limited by fluorophore photobleaching. (c) FRET distribution histograms for 70S complexes formed in the absence (left) and presence (right) of initiation factors. Adapted from Marshall et al. (2009), copyright © 2009 Cell Press, with permission from Elsevier.

a coordinated process that is directed by three initiation factors: IF1, IF2, and IF3. Following the initiation factor-mediated assembly of a 30S initiation complex (30S IC) bearing a P-site initiator fMet-tRNA<sup>fMet</sup> at an AUG start codon, joining of the 50S subunit is catalyzed by IF2 in its GTP-bound form (Laursen et al., 2005). This process, which results in the formation of a 70S initiation complex (70S IC) with fMet-tRNA<sup>fMet</sup> in the P site, has been studied using smFRET with the H101(Cy5)-h44(Cy3) inter-subunit labeling scheme described in Section IV (Figure 6.7) (Marshall et al., 2009). Delivery of H101(Cy5)50S subunits to h44(Cy3)30S ICs allowed real-time observation of subunit joining, an event signaled by a sharp transition from 0 to high FRET (Figures 6.15a and 6.15b). The mean FRET arrival time, which reports on the kinetics of 50S subunit joining, was  $31.3 \pm 7.3$  s in the absence of initiation factors, and  $5.6 \pm 0.9$  s in the presence of IF1, IF2, and IF3 (at 15 mM Mg<sup>2+</sup>). In addition to enhancing the rate of 70S IC formation, initiation factors were found to influence the conformational state in which the 70S IC is assembled. A bimodal FRET distribution with peaks centered at

$\sim 0.30$  and  $\sim 0.44$  FRET was observed (Figure 6.15c), with the  $\sim 0.44$ -FRET state representing the ribosomal conformation that is competent to bind the first EF-Tu(GTP)aa-tRNA ternary complex and enter into the elongation phase of translation. In the absence of initiation factors, little preference is shown toward assembly of the 70S IC in the  $\sim 0.44$ - versus the  $\sim 0.30$ -FRET state. However, addition of IF1, IF2, and IF3 leads to preferential formation of the 70S IC in the  $\sim 0.44$ -FRET state (Figure 6.15c), implying a role for initiation factors in guiding proper assembly of the 70S IC into its elongation-competent conformation during initiation.

### V.3 Translation Termination

In a similar manner, release factors (RFs) and the ribosome recycling factor (RRF) have been shown by smFRET to promote preferential population of particular conformations of the translational machinery, thereby guiding forward progression through the termination and recycling stages of protein synthesis (Sternberg et al., 2009). The

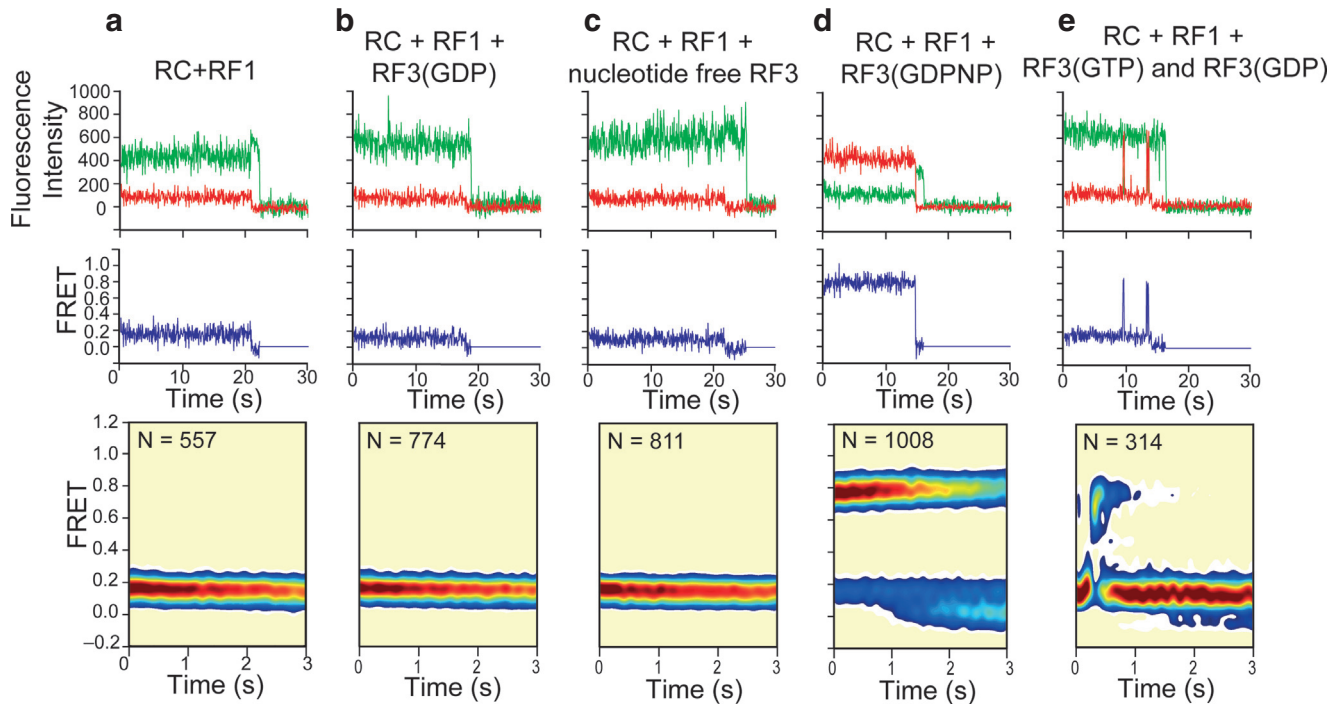


**FIGURE 6.16: Ribosomal conformational dynamics regulated by release factors during translation termination.** The  $D_5/A_5$  smFRET probes shown in Figure 6.7 were used to report on the dynamic equilibrium between GS1 and GS2 in ribosomal release complexes (RCs). (a) RC in the presence of  $1 \mu\text{M}$  RF1. Binding of RF1 blocks the GS1→GS2 transition and stabilizes GS1. (b) RF1-bound post-hydrolysis RC in the presence of  $1 \mu\text{M}$  RF3(GDP). (c) RF1-bound post-hydrolysis RC in the presence of  $1 \mu\text{M}$  nucleotide-free RF3. (d) Puromycin-treated RC in the presence of  $1 \mu\text{M}$  RF3(GDPNP). (e) RF1-bound post-hydrolysis RC with  $1 \mu\text{M}$  RF3 in the presence of a mixture of  $1 \text{ mM}$  GTP and  $1 \mu\text{M}$  GDP. Only those trajectories exhibiting fluctuations between GS1 and GS2 (42%) make up the time-synchronized contour plot (bottom row), which was generated by post-synchronizing the onset of the first GS1→GS2 transition event in each trajectory to time = 0.5 sec. Adapted from Sternberg et al. (2009), copyright © 2009 Nature Publishing Group, with permission from Macmillan Publishers Ltd.

termination of protein synthesis is signaled by the translocation of a stop codon into the A site, which is recognized by a class I RF (RF1 or RF2 in *E. coli*) that subsequently catalyzes hydrolysis of the nascent polypeptide from the P-site peptidyl-tRNA (Petry et al., 2008). This biochemical step generates a post-hydrolysis release complex (RC) with a deacylated tRNA at the P site. As described in Section IV, deacylation of P-site peptidyl-tRNA during elongation triggers large-scale fluctuations of the PRE complex. The presence of deacylated tRNA in the P site following RF1-catalyzed peptide release implies that the post-hydrolysis RC is intrinsically capable of analogous conformational fluctuations. The role of release and recycling factors in regulating these dynamics was assessed by monitoring their effect on the L1-tRNA smFRET signal, interpreted to report on transitions between the GS1 (low FRET, no L1-tRNA contact) and GS2 (high FRET, formation of L1-P/E-tRNA contact) global conformations of the ribosome.

In contrast to deacylation of the P-site tRNA via peptidyl transfer to puromycin or aa-tRNA during elongation, which results in stochastic fluctuations between GS1 and GS2, deacylation via RF1-catalyzed peptide release during termination generates post-hydrolysis RCs that are

locked in GS1. This finding suggests that RF1 binding blocks the GS1→GS2 transition. Indeed, addition of RF1 to puromycin-treated RCs suppresses fluctuations between GS1 and GS2, and shifts the  $\text{GS1} \rightleftharpoons \text{GS2}$  equilibrium predominately toward GS1 (Figure 6.16a). RF1 thus prevents fluctuations of the post-hydrolysis RC, which would otherwise occur spontaneously, and locks the ribosome in GS1 in anticipation of binding of the GTPase class II RF, RF3.

Biochemical experiments have suggested that RF3(GDP) binds to the RF1-bound RC, and that subsequent GDP-to-GTP exchange by ribosome-bound RF3 catalyzes the dissociation of RF1; GTP hydrolysis by RF3(GTP) then leads to its own dissociation from the RC (Zavialov et al., 2001). The role of the GS1→GS2 transition in this process has been demonstrated by a sequence of smFRET experiments using RF1, RF3, and various guanine nucleotides and their analogs (Figure 6.16). Neither addition of RF3(GDP) (Figure 6.16b) nor nucleotide-free RF3 (Figure 6.16c) to the RF1-bound, post-hydrolysis RC was capable of eliciting the GS1→GS2 transition. However, adding RF3(GDPNP) to a puromycin-treated RC traps it in GS2 (Figure 6.16d), suggesting that the GS1→GS2 transition occurs

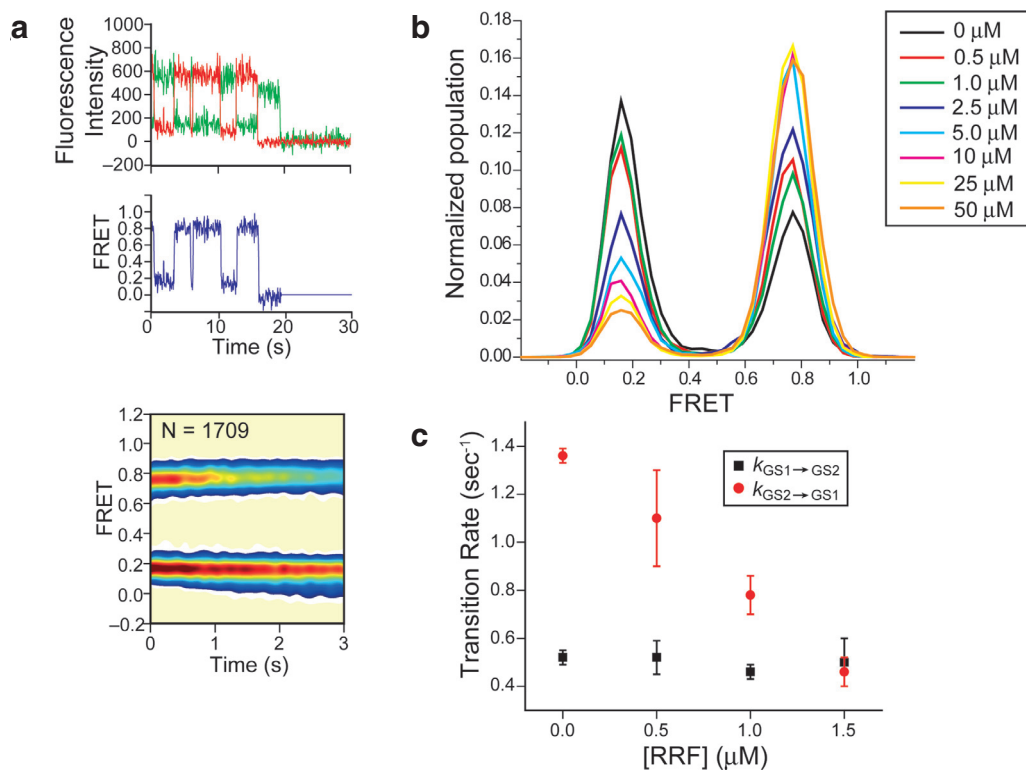


**FIGURE 6.17: Ribosome recycling factor fine-tunes the  $GS1 \rightleftharpoons GS2$  equilibrium within the post-termination complex.** The  $D_5/A_5$  probes shown in Figure 6.7 were used to report on the dynamic equilibrium between  $GS1$  and  $GS2$  in post-termination complexes (PoTCs). (a)  $Cy3/Cy5$  emission intensities, smFRET versus time trace, and contour plot of the time evolution of population FRET for PoTCs in the presence of  $1 \mu M$  RRF. (b) FRET distribution histograms of PoTCs as a function of RRF concentration. Low- and high-FRET states correspond to  $GS1$  and  $GS2$ , respectively. (c)  $k_{GS1 \rightarrow GS2}$  and  $k_{GS2 \rightarrow GS1}$  as a function of RRF concentration. Adapted from Sternberg et al. (2009), copyright © 2009 Nature Publishing Group, with permission from Macmillan Publishers Ltd.

concomitantly with, or subsequent to, GTP binding, but prior to GTP hydrolysis by RF3. In experiments where RF3(GDP) was added to RF1-bound post-hydrolysis RCs in a background of  $10 \mu M$  GDP,  $1 mM$  GTP, and  $1 \mu M$  RF1, multiple, short transitions from  $GS1$  to  $GS2$  could be observed in the smFRET versus time trajectories (Figure 6.16e), consistent with multiple rounds of RF3-catalyzed RF1 release followed by GTP hydrolysis/dissociation of RF3 and re-binding of RF1. Taken together, these results demonstrate that the  $GS1 \rightarrow GS2$  transition occurs only upon GTP binding to RF3. This change in ribosome global structure might occur spontaneously following RF1 dissociation, or alternatively, could serve as the driving force for RF1 release.

#### V.4 Ribosome Recycling

RF3-catalyzed release of RF1, followed by RF3 dissociation subsequent to GTP hydrolysis, generates a post-termination complex (PoTC) that is initially recognized by ribosome recycling factor (RRF). Subsequent splitting

of the PoTC into its constituent 30S and 50S subunits is catalyzed by the joint action of RRF and EF-G in a GTP-dependent reaction (Petry et al., 2008). The PoTC contains a deacylated tRNA in the P site and therefore is expected to exhibit dynamic  $GS1 \rightleftharpoons GS2$  fluctuations. Indeed, monitoring of PoTC dynamics using the L1-tRNA smFRET signal clearly demonstrates spontaneous transitions between  $GS1$  and  $GS2$ . Adding RRF to a PoTC was found to exert a subtle effect on the  $GS1 \rightleftharpoons GS2$  equilibrium, tilting occupancy toward  $GS2$  in an RRF concentration-dependent manner (Figure 6.17). At concentrations near the equilibrium dissociation constant of RRF for  $GS2$  ( $K_{d,GS2}$ ), this effect could be explained by a decrease in the rate of  $GS2 \rightarrow GS1$  transitions with increasing RRF concentration (Figure 6.17c). Considered in light of EF-G's known preference for  $GS2$ , this RRF-promoted shift toward higher fractional occupancy of  $GS2$  should favor EF-G(GTP) binding and thus splitting of the ribosomal subunits. This suggests that spatial or temporal variations in intracellular RRF concentrations could provide a means for regulating the efficiency of ribosome recycling in vivo. Regulation of the  $GS1 \rightleftharpoons GS2$

equilibrium thus appears to provide a common mechanism used by release and recycling factors to coordinate sequential biochemical events during the termination and recycling stages of protein synthesis. More generally, regulation of the ribosome's global state by translation factors serves to organize factor-binding events and biochemical steps over the course of the entire protein synthesis cycle.

## VI. CONCLUSIONS AND FUTURE DIRECTIONS

Investigation of the translational machinery by smFRET has allowed direct observation of large-scale conformational rearrangements of this universally conserved macromolecular machine. Through site-specific attachment of donor and acceptor fluorophores to the ribosome and its tRNA and translation factor ligands, specific conformational processes such as tRNA movements through the ribosome, inter-subunit rotation, and movements of the L1 stalk have been monitored in real time during the initiation, elongation, termination, and ribosome recycling phases of translation. Analysis of smFRET versus time trajectories collected under both pre-steady state and equilibrium conditions has allowed a detailed characterization of the kinetic and thermodynamic parameters underlying the dynamics of the translational machinery.

Collectively, these studies highlight the stochastic nature of individual steps within the mechanism of translation, in which thermal fluctuations of the ribosome and its tRNA substrates permit sampling of meta-stable conformational states on a complex multi-dimensional free-energy landscape (Munro et al., 2009c; Frank and Gonzalez, 2010). The preferred modes of thermally driven ribosomal motion, programmed into the ribosome's modular two-subunit architecture, may have been harnessed by the primordial ribosome to catalyze the essential reactions of protein synthesis – aa-tRNA selection, peptide bond formation, and translocation – long before the evolution of translation factors. Indeed, the contemporary ribosome can perform all of these functions, albeit slowly, to direct protein synthesis from an mRNA template in factor-free *in vitro* systems (Pestka, 1969; Gavrilova and Spirin, 1971; Gavrilova et al., 1976). The smFRET studies described in this chapter illustrate the ability of translation factors to regulate and direct conformational equilibria of the ribosome and its tRNA substrates during all stages of protein synthesis. Through the stabilization/destabilization of particular conformational states and the acceleration/deceleration of particular conformational transitions, a major mechanistic role of translation factors appears to be to guide the directionality of conformational processes intrinsic to the ribosome-tRNA complex. A particularly well-studied example is the ability of EF-G(GDPNP) to rectify stochastic conformational fluctuations of PRE complexes and to stabilize the

on-pathway translocation intermediate GS2, thereby facilitating and accelerating translocation. In an analogous way, smFRET characterization of the effect of ribosome-targeting antibiotics on the translational machinery's conformational dynamics has revealed that these drugs exert their inhibitory activities through the inhibition of the large-scale structural rearrangements that are required to drive protein synthesis.

Moving forward, many opportunities exist to apply the techniques described in this chapter to mobile ribosomal domains and conformational changes suggested by structural work, but not yet probed by smFRET. For example, an enhanced understanding of the function of the L7/L12 protein stalk of the 50S GTPase center, thought to recruit translation factors to the ribosome and facilitate biochemical steps such as GTP hydrolysis and  $P_i$  release (Mohr et al., 2002; Savelsbergh et al., 2005), would be greatly facilitated through characterization of the nature and timescale of its movements with respect to the ribosome, as well as the timing of its interactions with translation factors during the various stages of protein synthesis. Similarly, smFRET provides a means by which to characterize the kinetic and thermodynamic underpinnings of putative movements of the small subunit's head domain, which have been suggested to play an important role in regulating events during translation initiation (Carter et al., 2001), aa-tRNA selection (Ogle et al., 2002), and translocation (Spahn et al., 2004; Ratje et al., 2010). Efforts to obtain a complete mechanistic understanding of the conformational dynamics of the translating ribosome will benefit from the emergence of new technologies and experimental platforms. Recent advances, such as probing multiple conformational changes simultaneously using three-fluorophore labeling to investigate the degree of conformational coupling (Hohng et al., 2004; Munro et al., 2009a; Munro et al., 2009b), new illumination strategies permitting single-molecule detection in the presence of freely diffusing dye-labeled ligands at physiologically relevant micromolar concentrations (Levene et al., 2003; Uemura et al., 2010), and new data analysis algorithms permitting increasingly unbiased analysis of smFRET versus time trajectories (Bronson et al., 2009), will allow ever more complex mechanistic questions to be addressed. These techniques should prove particularly useful in the extension of smFRET techniques from the studies of Bacterial protein synthesis described here to the more complex and highly regulated translational machinery of higher organisms.

## ACKNOWLEDGMENTS

Work in the Gonzalez laboratory is supported by a Burroughs Wellcome Fund CABS Award (CABS 1004856), an NSF CAREER Award (MCB 0644262), an NIH-NIGMS grant (GM 084288–01), and an American Cancer Society Research Scholar Grant (RSG GMC-117152) to R.L.G.

We thank Joachim Frank, Dmitri Ermolenko, and Ilya Finkelstein for critically reading the chapter and providing valuable comments.

## REFERENCES

- Aitken, C. E. & Puglisi, J. D. (2010) Following the intersubunit conformation of the ribosome during translation in real time. *Nat Struct Mol Biol*, 17, 793–800.
- Andersen, C. B., Becker, T., Blau, M., Anand, M., Halic, M., Balar, B., Mielke, T., Boesen, T., Pedersen, J. S., Spahn, C. M., Kinzy, T. G., Andersen, G. R. & Beckmann, R. (2006) Structure of eEF3 and the mechanism of transfer RNA release from the E-site. *Nature*, 443, 663–8.
- Bergemann, K. & Nierhaus, K. H. (1983) Spontaneous, elongation factor G independent translocation of Escherichia coli ribosomes. *J Biol Chem*, 258, 15105–13.
- Blanchard, S. C., Gonzalez, R. L., Kim, H. D., Chu, S. & Puglisi, J. D. (2004a) tRNA selection and kinetic proofreading in translation. *Nat Struct Mol Biol*, 11, 1008–14.
- Blanchard, S. C., Kim, H. D., Gonzalez, R. L., Jr., Puglisi, J. D. & Chu, S. (2004b) tRNA dynamics on the ribosome during translation. *Proc Natl Acad Sci USA*, 101, 12893–8.
- Bretscher, M. S. (1968) Translocation in protein synthesis: a hybrid structure model. *Nature*, 218, 675–7.
- Brodersen, D. E., Clemons, W. M., Jr., Carter, A. P., Morgan-Warren, R. J., Wimberly, B. T. & Ramakrishnan, V. (2000) The structural basis for the action of the antibiotics tetracycline, pactamycin, and hygromycin B on the 30S ribosomal subunit. *Cell*, 103, 1143–54.
- Bronson, J. E., Fei, J., Hofman, J. M., Gonzalez, R. L., Jr. & Wiggins, C. H. (2009) Learning rates and states from biophysical time series: a Bayesian approach to model selection and single-molecule FRET data. *Biophys J*, 97, 3196–205.
- Carter, A. P., Clemons, W. M., Brodersen, D. E., Morgan-Warren, R. J., Wimberly, B. T. & Ramakrishnan, V. (2000) Functional insights from the structure of the 30S ribosomal subunit and its interactions with antibiotics. *Nature*, 407, 340–8.
- Carter, A. P., Clemons, W. M., Jr., Brodersen, D. E., Morgan-Warren, R. J., Hartsch, T., Wimberly, B. T. & Ramakrishnan, V. (2001) Crystal structure of an initiation factor bound to the 30S ribosomal subunit. *Science*, 291, 498–501.
- Cornish, P. V., Ermolenko, D. N., Noller, H. F. & Ha, T. (2008) Spontaneous intersubunit rotation in single ribosomes. *Mol Cell*, 30, 578–88.
- Cornish, P. V., Ermolenko, D. N., Staple, D. W., Hoang, L., Hickerson, R. P., Noller, H. F. & Ha, T. (2009) Following movement of the L1 stalk between three functional states in single ribosomes. *Proc Natl Acad Sci USA*, 106, 2571–6.
- Daviter, T., Gromadski, K. B. & Rodnina, M. V. (2006) The ribosome's response to codon-anticodon mismatches. *Biochimie*, 88, 1001–11.
- Dorner, S., Brunelle, J. L., Sharma, D. & Green, R. (2006) The hybrid state of tRNA binding is an authentic translation elongation intermediate. *Nat Struct Mol Biol*, 13, 234–41.
- Dorywalska, M., Blanchard, S. C., Gonzalez, R. L., Kim, H. D., Chu, S. & Puglisi, J. D. (2005) Site-specific labeling of the ribosome for single-molecule spectroscopy. *Nucleic Acids Res*, 33, 182–9.
- Draper, D. E. (2004) A guide to ions and RNA structure. *Rna*, 10, 335–43.
- Effraim, P. R., Wang, J., Englander, M. T., Avins, J., Leyh, T. S., Gonzalez, R. L., Jr. & Cornish, V. W. (2009) Natural amino acids do not require their native tRNAs for efficient selection by the ribosome. *Nat Chem Biol*, 5, 947–53.
- Ermolenko, D. N., Majumdar, Z. K., Hickerson, R. P., Spiegel, P. C., Clegg, R. M. & Noller, H. F. (2007a) Observation of intersubunit movement of the ribosome in solution using FRET. *J Mol Biol*, 370, 530–40.
- Ermolenko, D. N., Spiegel, P. C., Majumdar, Z. K., Hickerson, R. P., Clegg, R. M. & Noller, H. F. (2007b) The antibiotic viomycin traps the ribosome in an intermediate state of translocation. *Nat Struct Mol Biol*, 14, 493–7.
- Fei, J., Bronson, J. E., Hofman, J. M., Srinivas, R. L., Wiggins, C. H. & Gonzalez, R. L., Jr. (2009) Allosteric collaboration between elongation factor G and the ribosomal L1 stalk directs tRNA movements during translation. *Proc Natl Acad Sci USA*, 106, 15702–7.
- Fei, J., Kosuri, P., Macdougall, D. D. & Gonzalez, R. L., Jr. (2008) Coupling of ribosomal L1 stalk and tRNA dynamics during translation elongation. *Mol Cell*, 30, 348–59.
- Fei, J., Wang, J., Sternberg, S. H., Macdougall, D. D., Elvekrog, M. M., Pulukkunat, D. K., Englander, M. T. & Gonzalez, R. L., Jr. (2010) A highly purified, fluorescently labeled in vitro translation system for single-molecule studies of protein synthesis. *Methods Enzymol*, 472, 221–59.
- Feldman, M. B., Terry, D. S., Altman, R. B. & Blanchard, S. C. (2010) Aminoglycoside activity observed on single pre-translocation ribosome complexes. *Nat Chem Biol*, 6, 54–62.
- Frank, J. & Agrawal, R. K. (2000) A ratchet-like inter-subunit reorganization of the ribosome during translocation. *Nature*, 406, 318–22.
- Frank, J., Gao, H., Sengupta, J., Gao, N. & Taylor, D. J. (2007) The process of mRNA-tRNA translocation. *Proc Natl Acad Sci USA*, 104, 19671–8.
- Frank, J. & Gonzalez, R. L. (2010) Structure and dynamics of a processive Brownian motor: the translating ribosome. *Annual Review of Biochemistry*, 79, 9.1–9.32.
- Gavrilova, L. P., Kostishkina, O. E., Kotliansky, V. E., Rutkevitch, N. M. & Spirin, A. S. (1976) Factor-free (“non-enzymic”) and factor-dependent systems of translation of polyuridylic acid by Escherichia coli ribosomes. *J Mol Biol*, 101, 537–52.
- Gavrilova, L. P. & Spirin, A. S. (1971) Stimulation of “non-enzymic” translocation in ribosomes by p-chloromercuribenzoate. *FEBS Lett*, 17, 324–6.
- Gonzalez, R. L., Jr., Chu, S. & Puglisi, J. D. (2007) Thiostrepton inhibition of tRNA delivery to the ribosome. *Rna*, 13, 2091–7.
- Grosjean, H. J., De Henau, S. & Crothers, D. M. (1978) On the physical basis for ambiguity in genetic coding interactions. *Proc Natl Acad Sci USA*, 75, 610–4.
- Ha, T., Rasnik, I., Cheng, W., Babcock, H. P., Gauss, G. H., Lohman, T. M. & Chu, S. (2002) Initiation and re-initiation of DNA unwinding by the Escherichia coli Rep helicase. *Nature*, 419, 638–41.
- Harms, J. M., Wilson, D. N., Schluenzen, F., Connell, S. R., Stachelhaus, T., Zaborowska, Z., Spahn, C. M. & Fucini, P.

- (2008) Translational regulation via L11: molecular switches on the ribosome turned on and off by thiostrepton and micrococin. *Mol Cell*, 30, 26–38.
- Hickerson, R., Majumdar, Z. K., Baucom, A., Clegg, R. M. & Noller, H. F. (2005) Measurement of internal movements within the 30 S ribosomal subunit using Forster resonance energy transfer. *J Mol Biol*, 354, 459–72.
- Hohng, S., Joo, C. & Ha, T. (2004) Single-molecule three-color FRET. *Biophys J*, 87, 1328–37.
- Hopfield, J. J. (1974) Kinetic proofreading: a new mechanism for reducing errors in biosynthetic processes requiring high specificity. *Proc Natl Acad Sci USA*, 71, 4135–9.
- Horan, L. H. & Noller, H. F. (2007) Intersubunit movement is required for ribosomal translocation. *Proc Natl Acad Sci USA*, 104, 4881–5.
- Katunin, V. I., Savelsbergh, A., Rodnina, M. V. & Wintermeyer, W. (2002) Coupling of GTP hydrolysis by elongation factor G to translocation and factor recycling on the ribosome. *Biochemistry*, 41, 12806–12.
- Kim, H. D., Puglisi, J. D. & Chu, S. (2007) Fluctuations of transfer RNAs between classical and hybrid states. *Biophys J*, 93, 3575–82.
- Korostelev, A. & Noller, H. F. (2007) The ribosome in focus: new structures bring new insights. *Trends Biochem Sci*, 32, 434–41.
- Laursen, B. S., Sorensen, H. P., Mortensen, K. K. & Sperling-Petersen, H. U. (2005) Initiation of protein synthesis in bacteria. *Microbiol Mol Biol Rev*, 69, 101–23.
- Lee, T. H., Blanchard, S. C., Kim, H. D., Puglisi, J. D. & Chu, S. (2007) The role of fluctuations in tRNA selection by the ribosome. *Proc Natl Acad Sci USA*, 104, 13661–5.
- Levene, M. J., Korlach, J., Turner, S. W., Foquet, M., Craighead, H. G. & Webb, W. W. (2003) Zero-mode waveguides for single-molecule analysis at high concentrations. *Science*, 299, 682–6.
- Marshall, R. A., Aitken, C. E. & Puglisi, J. D. (2009) GTP hydrolysis by IF2 guides progression of the ribosome into elongation. *Mol Cell*, 35, 37–47.
- Marshall, R. A., Dorywalska, M. & Puglisi, J. D. (2008) Irreversible chemical steps control intersubunit dynamics during translation. *Proc Natl Acad Sci USA*, 105, 15364–9.
- Moazed, D. & Noller, H. F. (1989a) Interaction of tRNA with 23S rRNA in the ribosomal A, P, and E sites. *Cell*, 57, 585–97.
- Moazed, D. & Noller, H. F. (1989b) Intermediate states in the movement of transfer RNA in the ribosome. *Nature*, 342, 142–8.
- Mohr, D., Wintermeyer, W. & Rodnina, M. V. (2002) GTPase activation of elongation factors Tu and G on the ribosome. *Biochemistry*, 41, 12520–8.
- Munro, J. B., Altman, R. B., O'Connor, N. & Blanchard, S. C. (2007) Identification of two distinct hybrid state intermediates on the ribosome. *Mol Cell*, 25, 505–17.
- Munro, J. B., Altman, R. B., Tung, C. S., Cate, J. H., Sanbonmatsu, K. Y. & Blanchard, S. C. (2009a) Spontaneous formation of the unlocked state of the ribosome is a multistep process. *Proc Natl Acad Sci USA*, 107, 709–14.
- Munro, J. B., Altman, R. B., Tung, C. S., Sanbonmatsu, K. Y. & Blanchard, S. C. (2009b) A fast dynamic mode of the EF-G-bound ribosome. *Embo J*, 29, 770–81.
- Munro, J. B., Sanbonmatsu, K. Y., Spahn, C. M. & Blanchard, S. C. (2009c) Navigating the ribosome's metastable energy landscape. *Trends Biochem Sci*, 34, 390–400.
- Nikulina, A., Eliseikina, I., Tishchenko, S., Nevskaya, N., Davydova, N., Platonova, O., Piendl, W., Selmer, M., Liljas, A., Drygin, D., Zimmermann, R., Garber, M. & Nikonov, S. (2003) Structure of the L1 protuberance in the ribosome. *Nat Struct Biol*, 10, 104–8.
- Odom, O. W., Picking, W. D. & Hardesty, B. (1990) Movement of tRNA but not the nascent peptide during peptide bond formation on ribosomes. *Biochemistry*, 29, 10734–44.
- Ogle, J. M., Murphy, F. V., Tarry, M. J. & Ramakrishnan, V. (2002) Selection of tRNA by the ribosome requires a transition from an open to a closed form. *Cell*, 111, 721–32.
- Parker, J. (1989) Errors and alternatives in reading the universal genetic code. *Microbiol Rev*, 53, 273–98.
- Pestka, S. (1969) Studies on the formation of transfer ribonucleic acid-ribosome complexes. VI. Oligopeptide synthesis and translocation on ribosomes in the presence and absence of soluble transfer factors. *J Biol Chem*, 244, 1533–9.
- Petry, S., Weixlbaumer, A. & Ramakrishnan, V. (2008) The termination of translation. *Curr Opin Struct Biol*, 18, 70–7.
- Pioletti, M., Schlunzen, F., Harms, J., Zarivach, R., Gluhmann, M., Avila, H., Bashan, A., Bartels, H., Auerbach, T., Jacobi, C., Hartsch, T., Yonath, A. & Franceschi, F. (2001) Crystal structures of complexes of the small ribosomal subunit with tetracycline, edeine and IF3. *Embo J*, 20, 1829–39.
- Ratje, A. H., Loerke, J., Mikolajka, A., Brunner, M., Hildebrand, P. W., Starosta, A. L., Donhofer, A., Connell, S. R., Fucini, P., Mielke, T., Whitford, P. C., Onuchic, J. N., Yu, Y., Sanbonmatsu, K. Y., Hartmann, R. K., Penczek, P. A., Wilson, D. N. & Spahn, C. M. (2010) Head swivel on the ribosome facilitates translocation by means of intra-subunit tRNA hybrid sites. *Nature*, 468, 713–6.
- Rodnina, M. V., Gromadski, K. B., Kothe, U. & Wieden, H. J. (2005) Recognition and selection of tRNA in translation. *FEBS Lett*, 579, 938–42.
- Rodnina, M. V., Savelsbergh, A., Katunin, V. I. & Wintermeyer, W. (1997) Hydrolysis of GTP by elongation factor G drives tRNA movement on the ribosome. *Nature*, 385, 37–41.
- Rodnina, M. V. & Wintermeyer, W. (2001) Ribosome fidelity: tRNA discrimination, proofreading and induced fit. *Trends Biochem Sci*, 26, 124–30.
- Savelsbergh, A., Katunin, V. I., Mohr, D., Peske, F., Rodnina, M. V. & Wintermeyer, W. (2003) An elongation factor G-induced ribosome rearrangement precedes tRNA-mRNA translocation. *Mol Cell*, 11, 1517–23.
- Savelsbergh, A., Mohr, D., Kothe, U., Wintermeyer, W. & Rodnina, M. V. (2005) Control of phosphate release from elongation factor G by ribosomal protein L7/12. *Embo J*, 24, 4316–23.
- Schmeing, T. M. & Ramakrishnan, V. (2009) What recent ribosome structures have revealed about the mechanism of translation. *Nature*, 461, 1234–42.
- Schmeing, T. M., Voorhees, R. M., Kelley, A. C., Gao, Y. G., Murphy, F. V. T., Weir, J. R. & Ramakrishnan, V. (2009) The crystal structure of the ribosome bound to EF-Tu and aminoacyl-tRNA. *Science*, 326, 688–94.

- Spahn, C. M., Gomez-Lorenzo, M. G., Grassucci, R. A., Jorgensen, R., Andersen, G. R., Beckmann, R., Penczek, P. A., Ballesta, J. P. & Frank, J. (2004) Domain movements of elongation factor eEF2 and the eukaryotic 80S ribosome facilitate tRNA translocation. *Embo J*, 23, 1008–19.
- Spirin, A. S. (1968) How does the ribosome work? A hypothesis based on the two subunit construction of the ribosome. *Curr Mod Biol*, 2, 115–27.
- Spirin, A. S. (1985) Ribosomal translocation: facts and models. *Prog Nucleic Acid Res Mol Biol*, 32, 75–114.
- Stanley, R. E., Blaha, G., Grodzicki, R. L., Strickler, M. D. & Steitz, T. A. (2010) The structures of the anti-tuberculosis antibiotics viomycin and capreomycin bound to the 70S ribosome. *Nat Struct Mol Biol*, 17, 289–93.
- Stapulionis, R., Wang, Y., Dempsey, G. T., Khudaravalli, R., Nielsen, K. M., Cooperman, B. S., Goldman, Y. E. & Knudsen, C. R. (2008) Fast in vitro translation system immobilized on a surface via specific biotinylation of the ribosome. *Biol Chem*, 389, 1239–49.
- Steitz, T. A. (2008) A structural understanding of the dynamic ribosome machine. *Nat Rev Mol Cell Biol*, 9, 242–53.
- Sternberg, S. H., Fei, J., Prywes, N., Mcgrath, K. A. & Gonzalez, R. L., Jr. (2009) Translation factors direct intrinsic ribosome dynamics during translation termination and ribosome recycling. *Nat Struct Mol Biol*, 16, 861–8.
- Subramanian, A. R. & Dabbs, E. R. (1980) Functional studies on ribosomes lacking protein L1 from mutant *Escherichia coli*. *Eur J Biochem*, 112, 425–30.
- Sytnik, A., Vladimirov, S., Jia, Y., Li, L., Cooperman, B. S. & Hochstrasser, R. M. (1999) Peptidyl transferase center activity observed in single ribosomes. *J Mol Biol*, 285, 49–54.
- Taylor, D. J., Nilsson, J., Merrill, A. R., Andersen, G. R., Nissen, P., & Frank, J. (2007) Structures of modified eEF2 80S ribosome complexes reveal the role of GTP hydrolysis in translocation. *Embo J*, 26, 2421–31.
- Thompson, R. C. & Stone, P. J. (1977) Proofreading of the codon-anticodon interaction on ribosomes. *Proc Natl Acad Sci USA*, 74, 198–202.
- Traut, R. R. & Monro, R. E. (1964) The puromycin reaction and its relation to protein synthesis. *J Mol Biol*, 10, 63–72.
- Uemura, S., Aitken, C. E., Korlach, J., Flusberg, B. A., Turner, S. W. & Puglisi, J. D. (2010) Real-time tRNA transit on single translating ribosomes at codon resolution. *Nature*, 464, 1012–7.
- Valle, M., Zavialov, A., Sengupta, J., Rawat, U., Ehrenberg, M. & Frank, J. (2003) Locking and unlocking of ribosomal motions. *Cell*, 114, 123–34.
- Villa, E., Sengupta, J., Trabuco, L. G., Lebaron, J., Baxter, W. T., Shaikh, T. R., Grassucci, R. A., Nissen, P., Ehrenberg, M., Schulten, K. & Frank, J. (2009) Ribosome-induced changes in elongation factor Tu conformation control GTP hydrolysis. *Proc Natl Acad Sci USA*, 106, 1063–8.
- Wang, Y., Qin, H., Kudaravalli, R. D., Kirillov, S. V., Dempsey, G. T., Pan, D., Cooperman, B. S. & Goldman, Y. E. (2007) Single-molecule structural dynamics of EF-G-ribosome interaction during translocation. *Biochemistry*, 46, 10767–75.
- Yamada, T., Mizuguchi, Y., Nierhaus, K. H. & Wittmann, H. G. (1978) Resistance to viomycin conferred by RNA of either ribosomal subunit. *Nature*, 275, 460–1.
- Zavialov, A. V., Buckingham, R. H. & Ehrenberg, M. (2001) A posttermination ribosomal complex is the guanine nucleotide exchange factor for peptide release factor RF3. *Cell*, 107, 115–24.